



This project has received funding from the Euratom research and training programme 2014-2018 under grant agreement No 662287.



## EJP-CONCERT

European Joint Programme for the Integration of Radiation Protection Research

H2020 – 662287

# D9.106 – Guidelines for implementing the workplace geometry and the radiation field map in the dosimetry application

## Part 1: Workplace geometry

**Lead Authors:** Martin Andersson, Maria A. Duch, Jonathan Eakins, Jan Janssen, Pasquale Lombardo, Olivier van Hoey

**Reviewer(s):** Filip Vanhavere, Mercè Ginjaume  
and CONCERT coordination team

Work package / Task	<b>WP9</b>	<b>T9.6</b>	<b>SST 9.6.1.2</b>
Deliverable nature:	<b>Report</b>		
Dissemination level: (Confidentiality)	<b>PU</b>		
Contractual delivery date:	<b>2018-12-31 (M43)</b>		
Actual delivery date:	<b>M43</b>		
Version:	<b>1</b>		
Total number of pages:	<b>17</b>		
Keywords:	<b>Workplace geometry</b>		
Approved by the coordinator:	<b>M43</b>		
Submitted to EC by the coordinator:	<b>M43</b>		

**Disclaimer:**

The information and views set out in this report are those of the author(s). The European Commission may not be held responsible for the use that may be made of the information contained therein.

## Content

### PART 1: WORKPLACE GEOMETRY

<b>1</b>	<b>INTRODUCTION</b>	<b>4</b>
<b>2</b>	<b>INTERVENTIONAL RADIOLOGY WORKPLACES</b>	<b>4</b>
2.1	MODELLING THE OPERATING ROOM	5
2.2	GUIDELINES ON HOW TO SET-UP THE IPS SYSTEM	6
<b>3</b>	<b>MIXED NEUTRON-GAMMA WORKPLACE FIELDS</b>	<b>10</b>
3.1	MODELLING OF THE GEOMETRY	11
3.1.1	<i>PHE Neutron Facility</i>	13
3.2	GUIDELINES ON HOW TO SET-UP THE IPS SYSTEM	16
<b>4</b>	<b>CONCLUSIONS AND FUTURE WORKS</b>	<b>17</b>
<b>5</b>	<b>REFERENCES</b>	<b>17</b>

### PART 2: RADIATION FIELD MAPPING

<b>1</b>	<b>INTRODUCTION</b>	<b>21</b>
<b>2</b>	<b>INTERVENTIONAL RADIOLOGY WORKPLACES</b>	<b>21</b>
2.1	RADIATION FIELD: REQUIRED INFORMATION AND DATA SOURCES	21
2.1.1	<i>Required information</i>	22
2.1.2	<i>Data sources</i>	23
2.2	RADIATION FIELD LOOKUP TABLE APPROACH	27
2.3	RADIATION FIELD FAST MC SIMULATION APPROACH	28
2.4	SENSITIVITY STUDY ON PARAMETERS OF INFLUENCE	29
<b>3</b>	<b>MIXED GAMMA-NEUTRON WORKPLACE FIELDS</b>	<b>37</b>
3.1	RADIATION FIELD MAPPING	37
3.2	USE OF RADIATION MONITORS FOR NORMALIZATION	40
<b>4</b>	<b>CONCLUSIONS</b>	<b>42</b>
<b>5</b>	<b>REFERENCES</b>	<b>42</b>

## 1 Introduction

The objective of the PODIUM project is to develop a user-friendly online application to calculate workers' doses in real time. Instead of measuring individual doses with a physical dosimeter, doses will be calculated. This will be done by using a combination of (i) monitoring of the position of workers in real time and (ii) the simulation of the spatial radiation field, including its energy and angular distribution.

For this methodology, the geometry of the workplace is important since the accuracy of the position monitoring system of the workers will depend on how the system is implemented in each specific workplace; in particular, the placement of the tracking sensors is of great importance. In addition, some of the simulation modules would need a description of the workplaces (dimensions, construction materials...). This workplace description can be done once before the work starts, but it might need to be repeated if relevant elements of the workplace (like the shielding) are subject to change.

Another key aspect is the definition of the radiation field. To be able to simulate the staff doses many different parameters that allow to characterize its spatial, angular and energy distribution should be collected. The application of the proposed methodology for the radiation field mapping will be done in two fields that could most benefit of the advantages of it: interventional radiology and workplaces with mixed neutron/photon fields. Thus, the complexity of this task is different depending on the specific problem to simulate. In interventional radiology, the radiation field changes several times during a procedure of several hours in such a way a continuous calculation of the radiation field is required, whilst radiation fields for mixed neutron/photon workplaces are not that much time dependent. But even in this case the radiation field can vary, if the inventory or spatial positioning of radioactive sources in the workplace change over time. Therefore, the methodology for implementing the workplace geometry and the radiation field map in the dosimetry application are both of great importance.

The present document entitled "Guidelines for implementing the workplace geometry and the radiation field map in the dosimetry application. Part 1: Workplace geometry" describes the definition of the most important elements characterizing the workplaces geometry. The second part, which will be released later on during the development of PODIUM, will include the additional elements that will further improve the radiation field definition.

## 2 Interventional radiology workplaces

Interventional radiology and image-guided treatments are areas of the medical sector that could benefit from applying the PODIUM online dosimetry system. In these fields of application, it is foreseen to provide fast dose calculations by using two approaches. The first approach will use a library of pre-calculated dose conversion coefficients, while the second one will be based on the use of fast MC simulations with the MC-GPU code and calculations with standard codes such as PENELOPE.

The full description of the workplace geometry involves considering several elements present in the operating rooms, since the radiation field that reaches the worker position is mainly composed by scattered radiation produced when the radiation beam generated by the X-ray equipment impinges on the patient's body.

Therefore, information on different components is needed:

- Elements related to the generation of the X-ray beam:
  - o Anode (angle and material) of the X-ray tube.
  - o Inherent filtration of the X-ray tube (thickness and material).
  - o C-arm radius of the installed equipment (isocenter location).
  
- Elements that can influence the scattered radiation that reaches the worker' position:
  - o Anatomy of the patient (sex, height, weight), modelled by using anthropomorphic phantoms, as the main scattering body. Anatomical region examined (chest, abdomen, ...).
  - o Patient table (material, thickness, position).
  - o Characteristics and position of movable protective elements (table shields, ceiling-mounted or wall-mounted shields...).
  - o Focal spot position.
  - o Shape and size of the radiation field.
  - o Source to image intensifier distance.
  - o Source rotation angles.
  - o Image intensifier components.
  - o Source to walls/ceiling distance.
  - o Walls material.

Among these elements, the characteristics of the X-ray equipment installed in an operating room (X-ray tube, patient table, table shields...) could be considered as part of the workplace description, but in an interventional radiology procedure the operating conditions of this equipment will vary many times during the procedure. For instance, in a typical procedure the same X-ray tube will operate with different kilovoltages and added filtration, and the movable shields will be located at different places. This is why the geometrical description of all of these elements will be included in the future document "Guidelines for implementing the workplace geometry and the radiation field map in the dosimetry application. Part 2: Radiation field mapping" devoted on how to characterize the radiation field. In this section only the static elements of the room (walls, ceiling, shelves...) are considered for the workplace geometry definition in an interventional radiology room, since they will affect the placement of the tracking sensors. On the other hand, the materials and dimensions of the room walls have a very little impact on the staff doses and are not going to be included in the MC simulations.

The studied medical procedures are carried out in operating rooms that could have variable dimensions depending on the specific site, thus, in section II.1.1 it is proposed a method to model the operating room by using specific sensors in such a way that a CAD file is generated. This file could be used to easily visualize the geometry of the workplace with standard computer-aided design tools such as AutoCAD, and to define the relative positions of the most relevant elements in the room such as C-Arm, bed and shields. In section II.1.2 are included the guidelines on how to set-up the IPS system (see deliverable D9.105), specifically how to set the single camera system.

## 2.1 Modelling the operating room

The proposed method to model the operating room is to use Structure sensors (Occipital Inc.), i.e., a 3D camera attached on an iPad. The camera uses the RAM-memory to create a 3D mesh of the filmed geometry. The created 3D mesh environment was generated using the app Canvas. The 3D mesh is then post-processed by the additional "Scan To CAD" service (\$29.00 per scan) in the Canvas app, which converts the generated 3D mesh into an editable CAD file.



**Figure 1.** Print screen of the generated 3D mesh of the operating room using Structure sensors and the app Canvas.

To show the final outcome of the system, the process was applied to the operating room number 105 of the Malmö Hospital. The generated 3D mesh by the Canvas app and the post-process CAD file of the room are presented in Figure 1 and Figure 2.

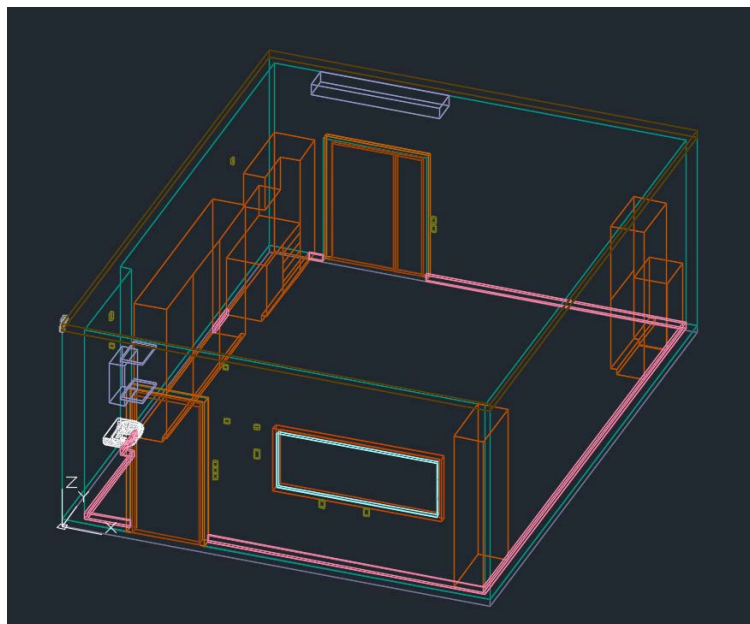


**Figure 2:** Post-processing CAD file of the operating room using the “Scan To CAD” service and shown in the computer software AutoCAD.

## 2.2 Guidelines on how to set-up the IPS System

The placement of the IPS camera is highly dependent on the features of the IR room where it is installed. For achieving an optimal tracking accuracy, the IPS camera should be placed following a series of ideal criteria, which are described in this paragraph. However, in some cases it could become necessary to compromise some criteria to reduce both the intrusiveness and the possibility of

obstructions. The first priority in the placement must be the discreteness of the IPS, i.e. we must assure that the work of the staff is not hindered during the course of any procedure. All the components of the IPS, including the Kinect, the cables and the acquisition PC controlling the IPS, must be placed safely and out of highly trafficked areas. This applies not only to the areas where doctor and nurses walk, but also to the areas where the C-Arm can be moved. Especially in the case of ceiling mounted C-Arms, it is necessary to take into account of the lateral excursion of the device when it is moved along its mounting rail.

Assuming that these requirements are met, the first condition for an optimal positioning is that the Kinect should have a front facing view of the staff. With a front facing view, the IPS will deliver the most accurate tracking of chest, head, and of both arms and both hands. To ensure that the tracking is continuous even when the doctor and the medical staff move around the patient, the Field Of View (FOV) must allow for coverage of a sufficiently large area (5-10 m<sup>2</sup>) surrounding the patient bed.

Considering the horizontal and vertical apertures of the RGB and depth sensors of the Kinect v.2, the ideal position should allow for a final distance between the Kinect and the doctor of about 2 to 4 meters. A distance of about 2.5/3 meters will deliver the highest tracking accuracy. Considering this constraint, the distance components along the longitudinal, lateral and vertical axes needs to be adjusted so that they respect some additional conditions. The vertical distance depends mostly on the height of the Kinect, and it has an obvious implication on the vertical inclination of the camera. The larger the vertical distance, the more downwards the Kinect will have to be rotated, so that the FOV reaches the doctor height. However, due to the inner limitation of the Kinect v.2 recognition algorithm, hard rotations about the horizontal axis (tilt angle) could lead to inaccuracies in the estimation of the joint's position. Above 25°, there is a high chance that bodies will not be recognized at all. In practical terms, the camera should not be placed above 2.5 meters of height. Similarly, also the horizontal rotation of the camera should not be too high. Hard rotations about the vertical axis of the camera can compromise the view of the doctor. The higher the horizontal rotation, the more lateral the view turns out to be. Lateral views can lead to self-occlusions, i.e. one side of the doctor's body hides the other side from the camera. In such cases, the Kinect recognition algorithm will try to infer the most probable position of the hidden joints. However, the joint inference algorithm can lead to negative effects on both precision and accuracy, and it can cause high frequency jittering to the hidden hand joint. Furthermore, high horizontal rotation angles will lead to difficulties in the calibration of the IPS. The calibration is a process through which we transform the local coordinates produced by the Kinect into Real-World coordinates, which are necessary for the calculation of the relative positions of source, patient, shields and doctor/nurse. For calibrating our IPS we make use of some reference patterns (checkered boards) that are placed on the room walls. The patterns should lie perpendicularly to the camera view to deliver the best accuracy in the calibration. Ideally, to reduce the chance of self-occlusions and to ease the calibration process, the horizontal rotation angle should lie in the range of (-20°, +20°).

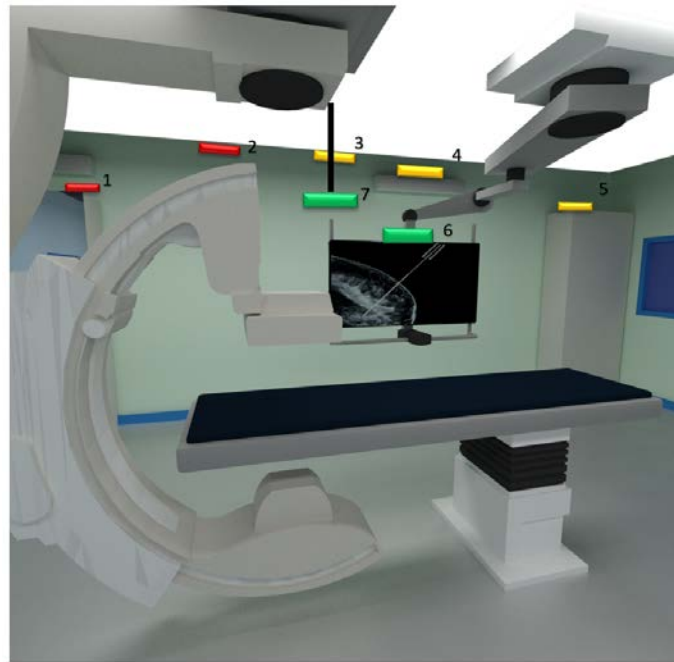


**Figure 3:** Potential Kinect locations within the Malmo test room. The most ideal positions are shown in green, while less favorable ones are indicated in orange and red.

Figure 3 shows some possible locations for the Kinect. The room geometry is taken from the Malmo Hospital test room number 105 (serving as reference in PODIUM), which has a ceiling mounted C-Arm from Siemens. In this figure, seven possible locations are shown. The green color code indicates the locations corresponding to the most ideal positions, while the red indicates the least favorable ones. The red locations would either deliver less accurate tracking data (increasing errors of about 1-2 cm), lead to frequent occlusions, or require a more complex calibration. Nevertheless, all these positions could be used in case the room geometry does not allow for placing the Kinect in the more ideal locations. Table 1 shows qualitative remarks with the respective advantages/drawbacks of each location.

Position	FOV	Distance Kinect-Doctor	Tilt angle	Horizontal angle	Occlusions	Calibration
<b>1: Kinect mounted on a closet on the side of the C-Arm.</b>	Good. It covers the whole region of interest.	Not good. The camera is far from the monitored area.	Good. The vertical position at about 2.1 m of height implies a tilt angle smaller than 20°.	Not good. The horizontal position requires angle of rotations larger than 20°.	High probability of occlusions with the C-Arm when rotated.	Complex due to large distances and relatively hard tilt and horizontal angles.
<b>2: Kinect hanging right below the ceiling on the same side of the C-Arm</b>	Good. It covers the whole region of interest.	Not good. The camera is far from the monitored area.	Not good. The vertical position at about 2.7 m of height implies a tilt angle higher than 25°.	Ideal. The Kinect has a front facing view of the doctor.	Medium probability of occlusion with C-Arm when rotated	Complex due to large distances and relatively hard vertical and horizontal angles.
<b>3: Kinect hanging right below the ceiling at the center of the bed</b>	Good. It covers the whole region of interest.	Good. The camera is not too far from the monitored area.	Not good. The vertical position at about 2.7 m of height implies a tilt angle higher than 25°.	Ideal. The Kinect has a front facing view of the doctor.	Low probability of occlusion from tv screen and C-Arm when rotated.	Easy, thanks to the ideal distances and to the relatively good vertical and horizontal angles.
<b>4: Kinect mounted on a wall light at about 2.3 meters of height</b>	Good. It covers the whole region of interest.	Not ideal. The camera is far from the monitored area.	Mediocre. The vertical position at about 2.3 m of height implies a tilt angle of about 20°.	Ideal. The Kinect has a front facing view of the doctor.	Medium probability of occlusion from tv screen and C-Arm when rotated.	Easy, thanks to the ideal distances and to the good vertical and horizontal angles.
<b>5: Kinect placed above the closet on the right side of the room</b>	Good. It covers the whole region of interest.	Not good. The camera is far from the monitored area.	Good. The vertical position at about 2.1 m of height implies a tilt angle smaller than 20°.	Not good. The horizontal position requires angle of rotations larger than 20°.	Medium probability of occlusion from tv screen if rotated.	Complex due to large distances and relatively hard vertical and horizontal angles.
<b>6: Kinect mounted on the imaging screen</b>	Excellent, doctor during procedure always look screen so even if moved it will always track doctor.	Excellent. The camera is at ideal distance to allow high accuracy and good view of the scene.	Good. The vertical position at about 2 m of height implies a tilt angle smaller than 20°.	Ideal. The Kinect has a front facing view of the doctor.	Very low risk of occlusions.	Complex. If the monitor is moved frequently, it will require an automated calibration procedure
<b>7: Kinect hanging on the ceiling thought a mounting rack</b>	Good. It covers the whole region of interest.	Excellent. The camera is at ideal distance to allow high accuracy and good view of the scene	Mediocre. The vertical position at about 2.2 m of height implies a tilt angle of about 20°.	Ideal. The Kinect has a front facing view of the doctor.	Very low risk of occlusions.	Easy, thanks to the ideal distances and relatively hard vertical and horizontal angles.

**Table 1: Comparison of advantages/drawbacks of the proposed locations for the placement of the camera in room 105 of Malmo Hospital**

To summarize:

1. Among all, locations 1 and 2 are the worst. Besides the hard angles (vertical and horizontal) and the high distances to the doctor, these positions are likely to lead partial occlusions when the C-Arm is rotated around the patient body. In this sense, position 5 is already a better option, but it can also lead to partial body occlusions because of the image monitor. However, in this case the camera is far from the monitored area, thus, reducing the useful tracking range and the accuracy of the depth measurement.
2. In principle, locations 6 and 7 deliver the best combinations of distances, FOV, rotation angles and occlusions risk-free. With such positions, in fact, the distances are maintained within 2 to 3 meters and the risk of self-occlusions and occlusions with objects is very low. However, the implementation of these setups presents some difficulties, reason for which we have not been able yet to place the Kinect in the Malmo test room. In the case of location 6, the problem is that the calibration will be invalidated when the doctor moves the monitor. This issue could be solved by means of an automatic calibration software re-calculating the transformation matrices when a change of position is detected. Within WP1, we will try to study the feasibility of developing an automated calibration software. On the other hand, by adopting the setup number 7 we would solve the issue of the calibration by means of a fixed holder hanging from the ceiling. In this case, we would have to leave an opportune clearance space between the C-Arm and the mounting rack, so that the camera will never interfere with the movements of the C-Arm. Therefore, in case the automatic calibration software reveals to be too difficult to be implemented for the setup number 6, we will consider the use of a fixed holder.
3. Overall, the locations 3 and 4 are the easiest to implement. The Kinect is far enough from the C-Arm, and the central position allows a frontal view of the doctor. So, even if the distances Kinect-doctor are relatively large, these Kinect locations still lead to a good tracking accuracy. The most concerning issues for these setups are the high tilt angle (especially in position 3, which can lead to a complex calibration) and to the risk of occlusions when the C-Arm is rotated towards the center of the bed.

### 3 Mixed neutron-gamma workplace fields

The PODIUM system is intended to be used in workplace fields that contain neutrons. However, due to the physical nature of neutron generation and of neutron-matter interactions, such fields will inevitably also contain photons. So, the system must in fact be suitable for dosimetry in mixed neutron-gamma fields, or at least it must be able to discriminate between neutron and gamma dose contribution.

Example scenarios where such fields can exist include, but need not be limited to:

- a. nuclear power stations and their associated support facilities, such as fuel processing, transport, and de-commissioning industries;
- b. accelerator facilities that have beam types and energies capable of producing neutrons as either primary or generated particles, such as might occur within high-energy research accelerators or around medical accelerators;
- c. engineering applications that utilize neutrons, such as for geological analyses of samples.

Within the scope of the PODIUM project, suitability of the system in the above types of field will be tested at two sites. The first is within the Radiation Metrology laboratory facility at PHE's Centre for Radiation, Chemical and Environmental Hazards (CRCE) in Chilton, UK. At this site, the low-scatter environment routinely used to perform Secondary Standards certified exposures to an  $^{241}\text{Am}$ -Be source has been modified by the inclusion of water tanks to produce a location- and angle-dependent field

that has been shown to be similar in energy distribution to the types of workplace fields that can exist at a nuclear power station.

The second is within a nuclear facility hosted at the SCK•CEN site in Mol, Belgium. At this facility, a transport container with spent MOX fuel will be placed in a large room. This setup represents a realistic mixed neutron/gamma workplace field in which workers can receive significant neutron dose.

### 3.1 Modelling of the geometry

In mixed neutron/photon workplace fields, the geometry and the radiation field are often coupled because the sources are often movable (e.g. transport containers with spent fuel, portable neutron sources ...). Therefore, in this first part of the deliverable both geometry and radiation field will be discussed. However, more details on the radiation field will be included in the second part of the deliverable.

The geometry of mixed neutron/photon workplace fields needs to include objects/materials that emit radiation or that can significantly influence the staff doses. For complex fixed radiation sources such as nuclear reactors or accelerators, usually simulations of the radiation field are already available for locations with significant dose rates. The data from these simulations can then be used to characterize the radiation field (e.g. as a phase space file) and the complex geometry of these sources need not to be included in the workplace geometry. For more simple portable radiation sources such as transport containers with spent fuel or portable neutron sources, a (simplified) model of the source should be included in the geometry and it should be possible to easily adapt the position of such sources and assessing the effect on the radiation field. Different objects/materials in the workplace can affect the radiation field by shielding or scattering. We will need to assess which objects/materials significantly affect the radiation field. The most important objects/materials need then to be included in the workplace geometry. For simple geometries this can be done by using simple macro-bodies. For more complex geometries, it might be necessary to use a CAD model. If a CAD model is not yet available it might be generated for instance by using the technique described in II.1.

In principle, the model of the facility needs to be sufficiently detailed to provide an accurate estimate of the dose rate at every location at which an individual might conceivably be located within it. The transient nature of the field would also need to be considered in environments in which that is relevant, such as fuel storage facilities, for example, where the inventory and spatial positioning of radioactive sources in the area might change over time. The model also needs to be robust to the inevitable uncertainty in accounting for every factor that could contribute to perturbations in the dose rate as a function of location, noting that some of these might conceivably be unknown or unknowable to the individual performing the modelling.

In practice, the above requirements would be impossible to fulfil completely. It is therefore clearly not realistic to provide precise and universal guidelines that are true in general on how to model a facility; instead, different requirements would necessarily be adopted and adapted on a case-by-case basis. However, several overall approaches may be adopted to mitigate against the problems caused by imprecise or incomplete knowledge of the input required for the model, and standard good practice will help to optimize the reliability of the results obtained:

#### **Simulation code:**

The simulation code used to generate the dose rate data can be either deterministic or Monte Carlo, general-purpose or user-specific. The only condition is that it needs to be fit for purpose, and hence able to output accurate data that is reliable for both neutrons and photons. This requirement may be demonstrated via independent testing and benchmarking. FLUKA, GEANT, MCNP and PHITS are examples of general-purpose Monte Carlo codes that fulfil these requirements, and can be considered

sufficiently consistent for the needs of the PODIUM system. It is not envisaged that advanced IT facilities, such as computer clusters, would be required to perform the simulations; the Monte Carlo codes listed above can easily all be run on standard PCs, though computational times would scale with the physical size and complexity of the site being modelled. It is necessary to run Monte Carlo calculations in coupled neutron-photon mode, with kerma conditions generally assumed such that electron transport may be neglected.

**Modeller:**

The accuracy of the dose rate map will clearly depend on the ability of the individual performing the modelling: it is obvious that they must be sufficiently familiar with mathematical modelling techniques to not only be able to construct a reliable model of the facility but also understand the uncertainties and limitations associated with their approach. This would include an awareness of parameter-sensitivity analyses, and an ability to determine which factors (e.g. objects, materials, physical parameters etc.) within their facility would be most key to obtaining accurate results. Whilst official accreditation of this discipline does not currently exist, competency could potentially be verified by a CV-based approach: demonstrably significant experience in mathematical modelling using the code to be employed, potentially alongside successful participation in intercomparison exercises, such as those organized periodically by the EURADOS WG6 consortium.

**Parameter variation:**

Even if a modeller could reproduce the geometry of their room with apparent high fidelity, there is still the possibility that 'hidden' aspects within it could impact dose rates. Examples here could be the unknown presence of neutron absorbing material behind a wall panel, which could significantly affect scatter, or imprecise knowledge of the material compositions or densities that they input into the model. It is therefore necessary to perform parameter sensitivity analyses of the modelled environment, to ascertain which factors are most and least significant. Furthermore, it is then necessary to benchmark the results against measured data. Estimates of ambient dose equivalent rates are suggested for this, because survey instruments are typically readily available within workplace fields. The recommended approach would be for the RPA to perform measurements at those locations that are judged to be the most susceptible to environmental factors, and also at those locations where individuals are most likely to be positioned during routine use of the facility, and compare their results with analogous data generated within the model; agreement between the measured and modelled results would support and confirm (or otherwise) the accuracy of the overall dose rate map. Given the energy-dependence of response of typical survey instruments, only broad confirmation may be possible.

**Time dependencies:**

It is possible that the geometry of the modelled room may be time-dependent, leading to a time-dependent dose rate map. It may therefore be necessary to produce a set of 'contingency' dose-rate maps for a given environment, each for a different anticipated configuration of objects within it, with the choice of which map is most appropriate to use made in real-time. The use of installed area monitoring equipment could also be employed to provide real-time dose assessments and correction factors

The above headings provide discussion on the general approach to modelling the geometry of a given neutron facility of interest. To illustrate the overall methodology, however, it is instructive to consider a case study that relates to the modelling of a real facility. This is provided below for the example of the PHE Radiation Metrology neutron laboratory, which contains an  $^{241}\text{Am}$ -Be source moderated by tanks of water as a simple simulation of a realistic workplace field within the nuclear industry (see next section). The second test with the transport container at SCK•CEN must still be started. In this case a simplified model of the room will be implemented in MCNP again by using macro-bodies. Also a simplified model of the transport container and the fuel will need to be implemented. Important in

this case will be that the position and orientation of the transport container can easily be modified. In MCNP this can be done for instance by specifying translations and rotations for the set of cells corresponding to the transport container. The simulations of the radiation field will then in principle need to be performed for a discrete set of possible positions of the transport container. If it is found that the radiation field is not influenced significantly by the materials in the room, the simulated radiation field can simply be translated and rotated together with the transport container and no additional simulations for different positions need to be performed. In that case it will also be easier to implement the presence of multiple transport containers.

### 3.1.1 PHE Neutron Facility

An image of the PHE neutron facility is shown in Figure 4. Cross-sectional and plan views of the PHE neutron facility are shown in Figure 5. The figure is schematic, being generated as output from a Monte Carlo model using the VISED package of MCNP. The laboratory is essentially a rectangular room, approximately 8 m long, 5 m wide, and 2.5 m high, with the source and exposure platform positioned on the central long-axis. When not in use, the  $^{241}\text{Am-Be}$  source is stored below ground, but is raised to a height of  $\sim 1.25$  m above the floor during exposures.



**Figure 4:** The PHE Neutron Laboratory in routine use. The  $^{241}\text{Am-Be}$  source is contained within a steel tube, itself partially encased within a lead shield (painted yellow). A moveable platform allows objects to be placed at different distances (and heights) along a central axis away from the source.

In order to build the model, measurements were made of the physical dimensions of every aspect of relevance within the real laboratory (Figure 4). Of course, ‘of relevance’ here is subjective, and is inevitably based on the judgement of the modeller. Nevertheless, it is evident (Figure 5) that aspects of the facility that were considered unlikely to affect the dose at a given location have not been included in the model; typical examples of this are small objects that may be judged not to induce significant neutron scatter, such as wall-fixtures, control panels, a monitor screen, and the wooden desk placed against the wall.

With all dimensions recorded, a scale diagram was produced that could subsequently be translated into the MCNP model. This translation proceeded according to standard methodologies used for Monte Carlo modelling projects: the geometry was deconstructed into a set of quadratic surfaces

defined and located according to an agreed coordinate system, with Boolean logic applied to then combine those surfaces into representations of the real-world shapes. In this case, the origin of the coordinate axes was identified with the 'standard' point-of-test used in routine measurements at PHE, which is 1 m from the source and 1.25 m above the floor, with the X-axis associated with the width of the room (left-right in Figure 5c), the Y-axis associated with the length of the room (left-right in Figure 5a, up-down in Figure 5c), and the Z-axis associated with the height of the room (up-down in Figure 5a). Pragmatically, the modelling was achieved using a text editor to create an MCNP-readable input file describing the geometry, with the VISED programme utilized to provide a visual double-check.

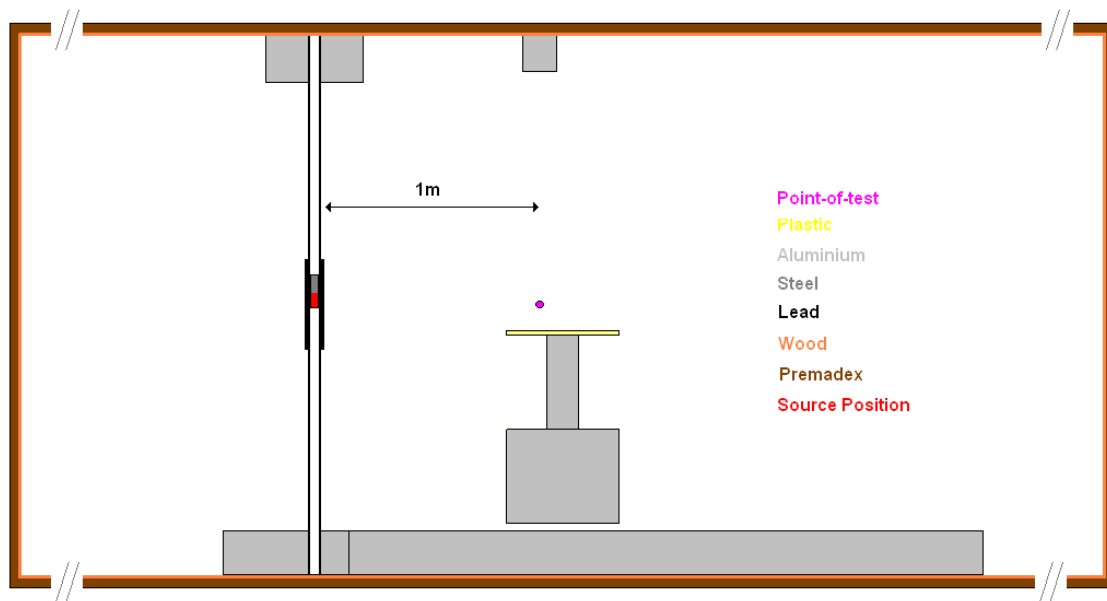


**Figure 5a:** Cross-sectional view of the PHE Neutron Laboratory in 'normal use'. The figure is truncated in the left-right direction: the actual laboratory is ~8m long (Y-axis) and ~2.5m high (Z-axis).

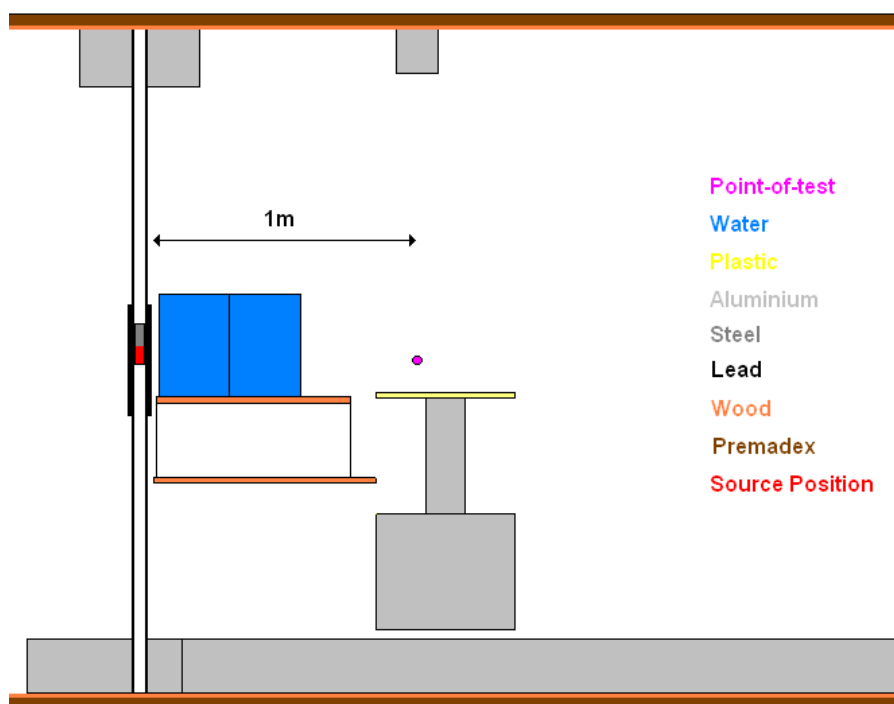


**Figure 5b:** Cross-sectional view of the PHE Neutron Laboratory including water tanks adjacent to the source.

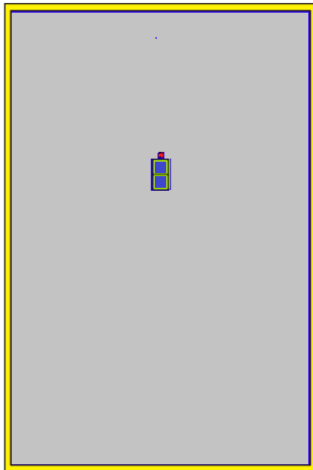


**Figure 5c:** Plan view of the PHE Neutron Laboratory. The water tanks are shown in blue, with the  $^{241}\text{Am-Be}$  source (red) positioned adjacently. The walls (yellow) incorporate wood panels placed in front of Premadex neutron-absorbing material. The laboratory is  $\sim 8\text{m}$  long (Y-axis) and  $\sim 5\text{m}$  wide (X-axis).

Once the spatial arrangements of objects had been defined, these shapes were ‘filled’ with the correct materials within the MCNP input file, in accordance with the physical objects present in the actual laboratory. MCNP considers matter as a ‘dense gas’, i.e. a mixture of isotopes (or atoms, for photon-only problems) in user-defined proportions. Essentially, a given material is therefore specified according to two main parameters: its physical density, given either as mass per volume or atoms per volume; and the ratio of its composite isotopes, given either as a mass-fraction or an atom-fraction. However, for neutron problems, a specification of the chemical bonding of light nuclei is also recommended, to correctly account for neutron-nucleus thermal scattering effects (i.e. the so-called  $S(\alpha,\beta)$  ‘thermal treatment’). For this third parameter for each material, the most up-to-date  $S(\alpha,\beta)$  data provided in MCNP were used, with the most appropriate next-best choice made where data were absent for a given material, such as using light water O-H data for tissue, or assuming polyethylene-like C-H bonds for wood, polymethyl methacrylate (PMMA), and Premadex ( $^6\text{Li}$ -loaded wax).

Of course, the accuracy of the model will depend on the accuracy with which the materials can be defined, which may be complicated if the precise chemical composition of a given object in a geometry is unknown. In such cases, best guesses and compromises would be inevitable. For the PHE laboratory, however, most of the materials used in its construction can be assumed to be fairly commonplace, such as the aluminium, stainless steel, lead, polymethyl methacrylate, wood and Premadex used to build the facility, and the water of the moderator. Typically, it was fairly easy to obtain physical density data from reliable and referenceable online sources for most common materials.

The chemical composition of common materials is also relatively easy to obtain. Of course, one complication to this for neutron exposures compared to photon-only problems is that the correct isotopic compositions of the individual elements in a given material need to be provided, alongside simply the ratio of elements in its chemical formula. For the most part, natural isotopic compositions were assumed for each element, freely obtainable from resources such as the “*Isotopic compositions of the elements*” [1]. Where non-standard isotopic compositions are relevant, such as for the Premadex neutron-absorbing material that is enriched with lithium-6 rather than natural lithium ( $\sim 10\% ^6\text{Li} + \sim 90\% ^7\text{Li}$ ), appropriate isotopic breakdown data provided by the manufacturers were used.

Once the shapes comprising the physical objects have been ‘filled’ with materials within the MCNP model, the specification of the geometry is essentially complete. However, the source term needs also to be defined within the model. For most workplace facilities where neutrons may be present, such as within the nuclear sector, the neutrons originate from a radioactive source of physical dimensions, density and material composition. Thus, source and geometry are effectively ‘coupled’ within Monte Carlo models containing neutrons, so the physical parameters of the source need to be incorporated into the specification of the input geometry. For the PHE source, this was relatively easy: the neutrons are emitted from a small cylinder of aluminium ( $\sim \text{few cm}^3$ ), inside of which the  $^{241}\text{Am-Be}$  is distributed

In addition to the physical specifications of the source, the energy distribution of the emitted neutrons needs to be defined within the model. Again, this is a relatively easy for the PHE  $^{241}\text{Am-Be}$  source, which is a well-defined calibration source that emits according to ISO 8529 [2] specifications. Moreover, MCNP normalizes all output results to 'per-source-particle'. In order to link that output to the real world, the activity of the source needs also to be considered, such that a multiplication factor may be introduced. As before, this is relatively easy for the PHE source, which is well-benchmarked and is calibrated to secondary standards criteria.

Similarly, to the specification of the material data, the accuracy of the model will depend on the accuracy with which the source term can be defined. For the PHE neutron facility model, the accuracy may therefore be assumed fairly high: the energy distribution of emitted neutrons and the composition of the source pellet are both well-known and well-characterized, with the dose rates at the point of test typically determined to better than 10 % uncertainty. In a general workplace environment, however, this may not be the case: the compositions and contents of fuel flasks, for example, may be known only to a limited extent, and the presence of short-lived radionuclides could lead to a transient emission characteristic. These limitations will lead to two related problems: firstly, the energy distributions of the neutrons and photons may be poorly known and time dependent; secondly, if the materials surrounding and shielding the source are poorly defined, the degree to which the neutrons are attenuated and secondary particles are generated may be simulated inaccurately by the model. The extent to which ignorance of the source term and its immediate environment will impact the dose rate at a given location will obviously vary on a case-by-case basis, but could be significant and again emphasizes the need for corroborative measurements and a cautionary approach to the modelling. This type of uncertainty will be investigated and discussed in later work, where application on the PODIUM system in an actual workplace field will be tested.

The MCNP simulation is run in coupled neutron-photon mode, with detailed physics options chosen by default. Of course, for the simulation to be useful, it is necessary to be able to extract results and output from it. The methodology applied to achieve this will be described in a later report, alongside discussions of attempts to mitigate for inaccuracy and uncertainty within the model.

### 3.2 Guidelines on how to set-up the IPS System

The main difficulties for mixed neutron/photon workplace fields arise from the fact that such workplaces can be very large and many workers can be present in one workplace. Therefore, often the use of two or even more tracking cameras will be required and the tracking algorithms need to be able to track all the workers present in the workplace.

Inevitably, use of the tracking cameras within a facility will vary on a case-by-case basis, with their number, locations and orientations fully dependent on the geography of the room and the objects within it, noting that these latter may potentially be variable. The objective would be for the cameras to be able to determine, at all times and for all anticipated configurations of the geography, the position and orientation of each individual within it. The minimum number and configuration of cameras is therefore that needed to achieve this aim in the environment in which the PODIUM system is to be employed. Essentially, this means that wherever an individual is and whatever might be around them (including other workers), there must always be a clear line-of-sight between him/her and at least one of the cameras. Depending on the tracking system used, additional cameras may also be required in very large environments, in the circumstance where individuals can move too far away from a given camera for his/her position or orientation to be accurately determined due to its finite range.

For a static environment, the camera configuration may be relatively straightforward: easily determinable given accurate scale-drawings and the stated field-of-view of the camera, and readily

testable post-installation. For transient environments, in which additional objects might be introduced or removed, the engineers and RPAs tasked with establishing the PODIUM system would need to carefully consider every conceivable permutation of objects within the room to ensure that line-of-sight is always possible. Again, annotatable scale-drawings of the environment, and thorough understanding of its intended operation, would be essential to guide this aim.

In all cases, safety systems must be put in place to ensure that any modifications from the set of configurations considered at the set-up stage would trigger a re-evaluation of the camera requirements. Obvious examples of this could be introducing new equipment into an environment, or re-purposing it so that it is no longer static. As always, the focus would be on the RPAs at such facilities to ensure that their dosimetry system is at all times fit for purpose.

For the case-study of the PHE Neutron laboratory, choosing the number and positioning of cameras may be relatively straight-forwards. This is because the laboratory is an approximately 5×8 m<sup>2</sup> rectangular room, with the neutron source, water moderating tanks, and calibration platform all located along the central axis, and no other significantly sized objects are present. Occlusions of individuals within the field-of-view can therefore only be caused by these central components or by the presence of other workers (if any) in the laboratory. The number of cameras in the room will likely scale with the number of workers, to ensure that there are no individual-individual occlusions. However if only one individual is likely to be present, which is the envisaged scenario in the PHE neutron facility, use of two tracking cameras may hypothetically be sufficient, because the only potential occlusion of that individual is by the moderating tanks.

The natural positioning of the two cameras would be in diagonally opposite corners of the room, assuming that each camera can track to a range of at least ~6 m and has a field of view of at least 90°. The door to the laboratory is at the bottom-right of Figure 5c, so the obvious locations of the cameras would therefore be in the bottom-left and top-right corners of Figure 5c. The suitability of these suggestions for the needs of the PODIUM system will be tested in due course.

## 4 Conclusions and future works

This document provides guidelines on how to model the workplaces according to the foreseen applications. These guidelines will be complemented with a future document “Guidelines for implementing the workplace geometry and the radiation field map in the dosimetry application.

Part 2: Radiation field mapping” devoted on how to characterize the radiation field. In the medical field the use of radiation shielding and operating conditions of the X-ray tube vary many times during an intervention, and this can have a big influence on staff doses. For mixed neutron-gamma workplaces the radiation field will be more easily described, but anyway should be calculated for each specific site every time it changes.

This work is ongoing and it will include both the methods to calculate the radiation field mapping and the description of the modelling of moving objects, for either interventional radiology workplaces: C-arm, protective shields; and mixed gamma-neutron workplaces: transport containers...

## 5 References

- [1] Commission on atomic weights and isotopic abundances, International Union of Pure and Applied Chemistry (IUPAC).
- [2] ISO 8529-1:2001. Reference neutron radiations - Part 1: Characteristics and methods of production.



This project has received funding from the Euratom research and training programme 2014-2018 under grant agreement No 662287.



## EJP-CONCERT

European Joint Programme for the Integration of Radiation Protection  
Research  
H2020 – 662287

# D 9.106 – Guidelines for implementing the workplace geometry and the radiation field map in the dosimetry application

## Part 2: Radiation Field Mapping

**Lead Authors:** Maria A. Duch, Jonathan Eakins, Jan T.M. Jansen, Pasquale Lombardo, Mahmoud Abdelrahman, Olivier van Hoey

**Reviewer(s):** Filip Vanhavere, Mercè Ginjaume  
and  
CONCERT coordination team

Work package / Task	WP9	T9.6	SST 9.6.1.2
Deliverable nature:	Report		
Dissemination level: (Confidentiality)	Public		
Contractual delivery date:	M49		
Actual delivery date:	M49		
Version:	1		
Total number of pages:	25		
Keywords:	Online dosimetry systems, indoor positioning system, radiation field mapping		
Approved by the coordinator:	M49		
Submitted to EC by the coordinator:	M49		

**Disclaimer:**

The information and views set out in this report are those of the author(s). The European Commission may not be held responsible for the use that may be made of the information contained therein.

## Content

### PART 2: RADIATION FIELD MAPPING

<b>1</b>	<b>INTRODUCTION</b>	<b>21</b>
<b>2</b>	<b>INTERVENTIONAL RADIOLOGY WORKPLACES</b>	<b>21</b>
2.1	RADIATION FIELD: REQUIRED INFORMATION AND DATA SOURCES	21
2.1.1	<i>Required information</i>	22
2.1.2	<i>Data sources</i>	23
2.2	RADIATION FIELD LOOKUP TABLE APPROACH	27
2.3	RADIATION FIELD FAST MC SIMULATION APPROACH	28
2.4	SENSITIVITY STUDY ON PARAMETERS OF INFLUENCE	29
<b>3</b>	<b>MIXED GAMMA-NEUTRON WORKPLACE FIELDS</b>	<b>37</b>
3.1	RADIATION FIELD MAPPING	37
3.2	USE OF RADIATION MONITORS FOR NORMALIZATION	40
<b>4</b>	<b>CONCLUSIONS</b>	<b>42</b>
<b>5</b>	<b>REFERENCES</b>	<b>42</b>

# 1 Introduction

The objective of the PODIUM project is to develop a user-friendly online application to calculate workers' doses in real time (Dosimetry Online Calculation Application, DCA). Instead of measuring individual doses with a physical dosimeter, doses will be calculated. Dose calculations will be performed based on two inputs: (i) the position of workers (in real time) and (ii) the spatial distribution of the radiation field, including its energy and angular distribution. On the one hand, the position of the worker is acquired by means of a tracking system based on depth cameras named IPS, i.e. Indoor Positioning System. On the other hand, the spatial distribution of the field is obtained by means of Monte Carlo simulations. This deliverable deals with the latter, i.e. the development of a methodology for simulating the radiation field.

A sufficiently accurate characterization of the radiation field in the workplace is crucial for a correct estimate of staff doses by simulation. Many parameters must be collected for allowing to characterizing spatial, angular and energy distributions of the radiation field. The application of the proposed methodology will be done in two fields that could benefit the most from our computational approach: interventional radiology and workplaces with mixed gamma neutron fields. Neutron fields are always mixed with photon radiation, however, in the framework of this project we will focus on the calculation of the neutron contribution of the mixed fields, because of its limitation with standard dosimetry techniques.

The complexity of this task is different depending on the specific problem to simulate. In interventional radiology, the radiation field changes several times during a procedure of several hours. Thus, for this application a continuous calculation of the radiation field is required, whilst radiation fields for mixed gamma-neutron workplaces are not much time dependent. But even in this case the radiation field can vary, therefore, it might be necessary to have an external dosimeter to scale the radiation field map proportional to this external dosimeter reading and use this as correction on temporal changes.

In Part 1 of this document, entitled "Guidelines for implementing the workplace geometry and the radiation field map in the dosimetry application. Part 1: Workplace geometry", the most important elements characterizing the workplaces geometry were described. The present document entitled "Guidelines for implementing the workplace geometry and the radiation field map in the dosimetry application. Part 2: Radiation Field Mapping" complements the previous document to describe the radiation field definition.

## 2 Interventional radiology workplaces

### 2.1 Radiation field: required information and data sources

Interventional radiology and image-guided treatments are the areas of the medical sector that could benefit the most from applying the PODIUM online dosimetry system. In these fields of application, it is foreseen to provide fast dose calculations by using two approaches. The first approach will use a library of pre-calculated conversion coefficients, while the second one will be based on the use of fast MC simulations with the MC-GPU code and other accelerated calculations with standard codes such as PENELOPE.

- The first approach is based on the use of two lookup tables:
  - a radiation field lookup table, which is used to define the distributions of photon intensity, energy and direction (angle), and
  - a dose conversion coefficient (DCC) lookup table, which defines organ doses for partial body irradiation with photons of a certain energy and direction.

The radiation field lookup table is developed within WP1 task 1.2, while the creation of the sets of dose conversion coefficients is part of WP2 of PODIUM.

The two tables will be integrated in a dedicated software (developed in WP3), named IPP\_SE, which is run remotely by the web application.

In the second approach, the radiation field at the position of the monitored worker is calculated “live” by the MC programme used in the dose calculation for each irradiation event.

### 2.1.1 Required information

The scattered radiation field should be calculated with clinic and patient specific data, but for both foreseen approaches (lookup table approach or direct MC simulation) the same basic information is needed. Some of these data correspond to the physical configuration of the X-ray tube and could be considered as fixed values for a specific room, and gathered during the setting-up of the dosimetry application in the facility, see Table 1.

**Table 1.** Fixed Information related to the generation of the X-ray beam and expected data source.

Required information	Data source
<b>X-ray tube characteristics</b>	
Anode (angle and material) of the X-ray tube	Manufacturer
Inherent filtration of the X-ray tube (thickness and material)	
<b>Examination room components</b>	
C-arm radius of the stand (i.e. isocenter location) 	Manufacturer
Image intensifier components 	
Patient table and mattress characteristics (material, thickness) or attenuation data 	Manufacturer or Experimental Measurements
Characteristics of movable protective elements (table shields, ceiling-mounted or wall-mounted shields...) 	Manufacturer

However there are patient specific data that have to be retrieved in real-time or at a minimum be available at the end of a procedure:

- Anatomy of the patient modelled by using anthropomorphic phantoms, as the main scattering body. The thickness of the exposed body, the main parameter, could be predicted knowing the weight, length, sex and age of the patient. This information should be introduced by the operator in the DCA.
- Anatomical region examined (chest, abdomen, ...), procedure type.
- For each projection/irradiation event:
  - Date/time it started, duration.
  - Focal spot position.
  - Shape and size of the radiation field.
  - Source to image intensifier distance.
  - Source rotation angles.
  - kVp (kV).
  - Added filtration.
  - Position of the reference point.
  - Dose at the reference point, for normalization purposes.
  - Position of movable protective elements (table shields, ceiling-mounted or wall-mounted shields...).
  - Patient's table position (x,y,z) in (cm).

### 2.1.2 Data sources

As described in "D 9.110 - Validation of the application in a controlled experiment set-up in a hospital", extracting the technical data from the x-ray machine was explored. The acquisition modality acquires the images, generate different reports, temporally store and send them to the Picture and Archiving System (PACS) following the DICOM protocol.

There are different data sources generated by the acquisition modality:

- Patient images. There is some information included in the DICOM-header files, but not all parameters needed.
- Radiation Dose Structured Report (RDSR). The document contains information arranged in a branching manner on different hierarchical levels that are linked to one another (XML structure), Figure 1.
- Modality-performed procedure steps (MPPS) report. Generated by the modality, can contain information about the examination, but there is a high variability of contents.
- Abbreviated Reports. There is some information included in the DICOM-header files, but not all parameters needed, Figure 2.

```
(0040,a010) RelationshipType CS # 8 1 [CONTAINS]
(0040,a040) ValueType CS # 4 1 [NUM ]
(0040,a043) ConceptNameCodeSequence SQ # 80 1
  (0008,0100) CodeValue SH # 6 1 [113790]
  (0008,0102) CodingSchemeDe... SH # 4 1 [DCM ]
  (0008,0104) CodeMeaning LO # 22 1 [Collimated Field Area ]
]
(0040,a300) MeasuredValueSequence SQ # 108 1
  (0040,08ea) MeasurementUni... SQ # 58 1
    (0008,0100) CodeValue SH # 2 1 [m2]
    (0008,0102) CodingSc... SH # 4 1 [UCUM]
    (0008,0104) CodeMeaning LO # 4 1 [m^2 ]
  ]
  (0040,a30a) NumericValue DS # 10 1 [0.0073935 ]
```

**Figure 1.** Excerpt of a RDSR (source: Skåne University Hospital)

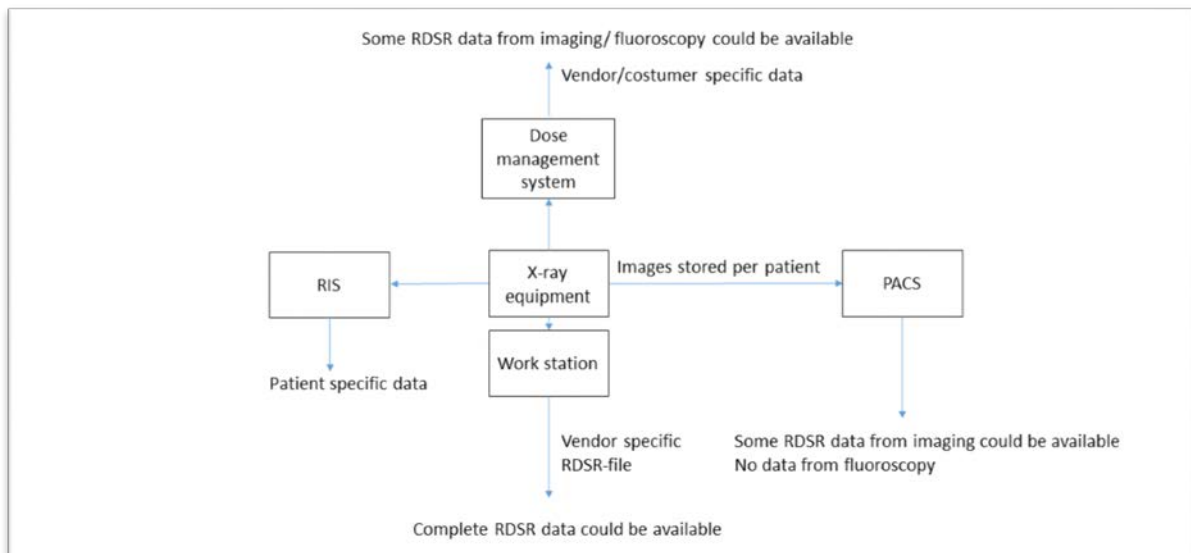
Report status:	Partial
Cumulative fluoroscopy time:	16.07 min:ss
Cumulative DAP (fluoroscopy):	514917 mGycm <sup>2</sup>
Cumulative DAP (exposure):	59243 mGycm <sup>2</sup>
Total DAP:	574160 mGycm <sup>2</sup>
Cumulative frontal Air Kerma:	681.80 mGy
Cumulative lateral Air Kerma:	0.00 mGy
Total number of acquired runs:	23
Total number of acquired images:	1305
Total number of acquired exposure images:	1222

Run no.	No. of Images	Procedure	Image Channel	Suprad. Fr / rate	AV	RA	WAS	AP	DA	DA' (mGycm <sup>2</sup> )	RAO (deg)	Rotat (deg)	Appt (cm)	SPD (cm)
1	71	Coronary 15fps Normal	Fr	15	74	724	6	3072	19.12	LA03	CAUD29	121		
2	80	Coronary 15fps Normal	Fr	15	74	750	7	3503	22.24	RA03	CAUD24	120		
3	82	Coronary 15fps Normal	Fr	15	72	669	6	2986	19.01	RA027	CRAN28	121		
4	81	Coronary 15fps Normal	Fr	15	70	516	6	2067	12.93	RA01	CRAN33	121		
5	80	Coronary 15fps Normal	Fr	15	84	763	8	6083	38.18	LA030	CRAN31	121		
6	70	Coronary 15fps Normal	Fr	15	83	772	8	3507	25.12	LA029	CAUD7	119		
7	71	Coronary 15fps Normal	Fr	15	81	793	8	4716	32.65	LA02	CRAN29	121		
8	50	Coronary 15fps Normal	Fr	15	79	813	7	3191	22.86	RA033	CRAN7	121		
9	72	Coronary 15fps Normal	Fr	15	90	736	8	5501	38.52	LA044	CAUD24	117		
10	40	Coronary 15fps Normal	Fr	15	74	752	7	1458	10.30	RA03	CRAN32	121		
11	52	Coronary 15fps Normal	Fr	15	90	739	8	4137	28.90	LA051	CAUD26	119		
12	52	Coronary 15fps Normal	Fr	15	72	628	6	1394	10.02	RA023	CRAN26	121		
13	6	Coronary 15fps Normal	Fr	15	71	606	6	204	1.99	LA01	CRAN28	121		
14	83	Fluoroscopy	Fr	15	76	10		287	1.47	LA01	CRAN28	121		
15	11	Coronary 15fps Normal	Fr	15	69	475	5	264	1.43	RA08	CRAN31	121		
16	46	Coronary 15fps Normal	Fr	15	73	674	6	1513	8.19	RA05	CRAN31	121		
17	53	Coronary 15fps Normal	Fr	15	71	615	6	1964	10.62	RA08	CRAN31	121		
18	8	Coronary 15fps Normal	Fr	15	70	549	6	229	1.4	RA08	CRAN31	121		
19	46	Coronary 15fps Normal	Fr	15	73	671	6	1671	9.01	RA05	CRAN31	121		
20	63	Coronary 15fps Normal	Fr	15	75	780	6	3599	19.29	RA05	CAUD30	120		
21	52	Coronary 15fps Normal	Fr	15	71	589	6	1705	9.21	RA09	CRAN29	120		
22	63	Coronary 15fps Normal	Fr	15	73	697	6	2731	14.70	RA09	CRAN29	121		
23	60	Coronary 15fps Normal	Fr	15	76	821	7	3746	20.06	RA09	CRAN32	121		

**Figure 2.** Example of abbreviated report (source: Saint James Hospital)

Other data sources, e.g. a dose management system, could contain the data in a structured manner. However, this is highly dependent on the hospital protocols. Figure 3 gives a schematic overview of data sources that could contain important data.



**Figure 3.** A schematic over view of where different machine data from a procedure are available.

name	manufacturer	data acquisition	site	user access	modalities
Agfa HealthCare Dose Monitoring, powered by tqmlDose™	Qaelum	RDSR, MPPS, OCR, header	local	web	CT, XA, DR, MG
Dose M™	Infinitt	RDSR, MPPS, OCR, header	local	web	CT, XA, DR, MG
Dose Monitor™	PACS Health	RDSR, MPPS, OCR	local	web	CT, XA, DR, MG
DoseIntelligence™	Pulmokard	RDSR, MPPS	cloud	web	CT, XA, DR, MG
DoseMetrix™	Primordial Design	RDSR, MPPS, OCR, header	local	web	CT, XA, DR, MG
DoseTrack™	Sectra	RDSR, MPPS, OCR	cloud	SA	CT, XA, DR, MG
DoseUtility™	Pixelmed Publishing Open source	RDSR, OCR	local	web	CT
DoseWatch™	GE Healthcare	RDSR, MPPS, header	local	web	CT, XA, DR, MG
DoseWatch explore™	GE Healthcare	eigener standard	cloud	web	CT <sup>1</sup>
DoseWise™	Philips	RDSR, MPPS, OCR, header	local	SA	CT, XA, DR, MG
Imalogix™	medInt Holdings LLC	RDSR, MPPS, OCR, header	cloud	web	CT, XA, DR, MG
Novadose™	Novarad	RDSR, MPPS, OCR	local	SA <sup>2</sup>	CT, XA, DR, MG
openREM™	The Royal Marsden NHS Foundation Trust (RMH), open source	RDSR, OCR, header	local	web	CT, XA, DR, MG
Radiance™	open source	RDSR, OCR	local	export, dashboard	CT
Radimetrics™	Bayer	RDSR, MPPS, OCR	local	web	CT, XA, DR, MG
Scannerside™	Drs. Talati, Moore of Rightdose, Inc.	RDSR, OCR	cloud	web	CT, XA
Teamply™	Siemens Healthcare	RDSR, OCR	cloud	web	CT, XA, DR, MG

CT: Computed tomography; XA: Angiography; DR: Digital radiography; MG: Mammography; SA: Standalone application, RDSR: DICOM Radiation Dose Structured Report; OCR: Optical Character Recognition; MPPS: Modality Performed Procedure Step; Header: DICOM-Header. This information was obtained from the manufacturers' websites or was furnished by the manufacturers themselves. The authors make no claims regarding the accuracy or completeness of the information. Other modalities such as nuclear medicine or digital volume tomography modalities as well as specific other data collection methods are not listed. The data for Siemens Teamply are taken from the white paper [46].

<sup>1</sup> GE-CT only.

<sup>2</sup> License from DoseMonitor™, integrated into the PACS and RIS.

**Figure 4.** Review of dose management systems characteristics (Boos et al, 2016).

In addition Figure 4, taken from a recent review (Boss et al, 2016), shows commercially available dose management systems. Most of them are based on the Radiation Dose structured Report and offer the possibility to export it in Excel format.

However, as mentioned before, the available system will be different for each hospital, and in particular, at Skåne University Hospital the DoseTrack system from Sectra is available, but at Saint James Hospital there is no dose management system available. Consequently, for the PODIUM project the preferred data source will be the RDSR.

Finally, at Skåne University Hospital the RDSR in DICOM format can be directly obtained from the work station of Siemens acquisition modalities whilst at Saint James Hospital, also from Siemens modalities, the data extraction was only possible in Excel format by using an application provided by the vendor. In all cases the RDSR-files are available from the work station only after each treatment finalizes.

For these reasons, the PODIUM dosimetry calculation application (DCA) has been developed (in WP3) to deal with the RDSR formats available at Skåne University Hospital and Saint James Hospital, where the PODIUM application will be tested (WP4). However, the DCA is structured so that it could be easily adapted to another RDSR output and also it could correctly deal with real-time information of the irradiation event (during the procedure).

In addition, it should be pointed out that the RDSR does not always contain all the required information for the dose calculation and, that, RDSRs from different vendors do not exactly match. Each vendor follows its own DICOM Conformance Statement. However, different x-ray machines from the same vendor comply with the same format (i.e. contain the same information data).

RDSR files from Skåne University Hospital and Saint James Hospital (from Siemens systems as has been mentioned before) have been revised to identify the available information, the information that can be determined even if it is not included in the RDSR, and the assumptions that can be made for the missing information. Table 2 summarizes the required information, identifies if it is directly available or, if needed, and not available, the proposed strategy to derive it. In addition, although it is not initially foreseen to use Philips systems in PODIUM, some RDSR files from Philips modalities were also studied for future improvements.

**Table 2.** Specific patient procedure and expected data source.

Required information	Available through the RDSR	Alternative method to derive it
Procedure type	✓	
Date/time started	✓	
Duration (ms)	✓	
Focal spot position (related to operator coordinates)	Not available	Indoor Positioning System
Size of the radiation field	Not available in Siemens systems, available for Philips	When missing, the value will be calculated by using the Dose Area Product, assuming a square field
Shape of the radiation field (position of the collimators)	Not available in Siemens systems, available for Philips	The field shape will be assumed to be squared
Source to image intensifier distance	✓	
Source rotation angles (Primary and Secondary angles)	✓	
kVp (kV)	✓	
Added filtration	Available for Siemens, not always available for Philips	The value can be gathered from the manufacturer, derived from the applied protocol
Position of the reference point	✓	
Dose at the reference point (Gy)	✓	
Dose area product (Gym <sup>2</sup> )	✓	
Patient's table position (x,y,z)	✓	
Position of movable protective elements (table shields, ceiling-mounted or wall-mounted shields...)	Not available	Specific positioning system (based on cameras or inertial movement sensors)

It should be commented that the X-ray console time stamp has to be synchronized with other equipment and programs, in particular with IPS output. The position of the table in lateral and longitudinal direction may be set to zero by the operator in order to set reference for an anatomical structure during the treatment. So, this zero position is not standardized and it is likely to vary with each room installation making it unusable as reference. However, for simulation purposes it can be sufficient to know the anatomical region of interest to position the patient's body.

## 2.2 Radiation field lookup table approach

The first of the two calculation approaches used in PODIUM is based on the creation of lookup tables comprising information of the radiation field and the organ dose conversion coefficients. This approach was established by PODIUM members as an intermediate step towards real-time simulations. This approach could still be useful in those cases where it is not feasible to perform fast simulations, because of the lack of a fast and stable internet connection to connect with the calculation server or because of the lack of high computational power in-situ, which is often the case in hospitals.

The radiation field lookup table includes the data used for characterizing the field in the so-called scatter sphere and ray tracing approach. The data are stored in a series of scatter fluence files corresponding to a fixed set of input source parameters, which include machine parameters (kVp, primary and secondary projections, filtration, focal spot position relatively to the patient body etc.) and types of patient body. Each scatter fluence file contains the energy spectrum of the photon fluence found on a sphere centered in the focal spot of the C-Arm.

The energy distribution of the fluence is computed by means of the MCNPx 2.70 transport code, using the F5 tally with the energy discrimination card DE. For the calculation, the surface of the sphere is approximated with small rectangular faces inscribed in the sphere. Each sphere is segmented in 2592 rectangular faces, i.e. one face every 5 degrees for both polar and azimuthal angles. Furthermore, depending on the distance between the doctor's body and the focus spot of the C-Arm, different sphere diameters are used. This allows to increase the accuracy of the dose calculation methodology, especially when the range of distances between the doctors body parts and the patient body varies from very close of the primary beam (0.5 m) to 1.5-2 meters far (for example, in case the pedal is used at distance during acquisitions and fluoroscopy moments). In order to reduce the extent of the radiation field lookup table, for the moment the PODIUM dosimetry system makes use of 2 sphere diameters for close-by and farther doctor body joints: 50 and 80 cm.

The radiation field lookup table containing the scatter fluence files is integrated in the dedicated software IPP\_SE, which is run directly by PODIUM's web-application. Besides handling the radiation field lookup table, IPP\_SE is also used for convoluting relevant parameters for the source definition with the tracking data, and thus to provide the dose calculation based on the dose conversion coefficient lookup table. In the DCC table, the anterior surface of the upper part of the phantom is subdivided in 6 rectangular faces, named Field Panels. The Field Panels are:

- 1) Top left/right covering head and neck,
- 2) Mid left/right covering the chest, and
- 3) Bottom left/right covering abdomen and pelvis).

In WP2, organ DCCs are calculated by irradiating one field panel per time with a parallel monoenergetic beam of photons impinging with a certain angle  $\theta$ .

The convolution between machine parameters (defining the radiation field), doctor position and posture is achieved through a ray tracing algorithm included in IPP\_SE. The algorithm 'traces' rays between the focal spot and the 6 field panels, calculates distances and incidence angles  $\theta$  between the focal spot and doctor body parts. The convolution links the calculated incidence angles with the corresponding energy distributions taken from the scatter fluence file. This information is then used to pick the correct organ dose conversion coefficient from the respective lookup table, for each field

panel. Finally, the intensity of the fluence is corrected by the DAP value (read from the RSDR) and reduced by a rescaling factor (<1) proportional to the distance between the field panel and the focal spot. This fluence rescaling factor is obtained on the basis of our validation and sensitivity studies, and it can be seen as an extension of the inverse square dependency of the intensity of a point source. The development of this algorithm is carried out together with the development of the dose conversion coefficient lookup table, and thus within WP2.

However, the size of the lookup table and thus the total number of scatter fluence files depends on relevant combination of input source parameters, which is assessed by means of a sensitivity study. For the first validation of the PODIUM dosimetry system, it was decided that the total number of scatter fluence files will be limited below the thousand cases. Nevertheless, it will be always possible to increase both the amount of fixed sets of input source parameters and the sphere diameters by means of future software update, should higher accuracy be needed. A sensitivity study has been performed to decide on the criteria to select the simulated sets for PODIUM (see II.4).

### 2.3 Radiation field fast MC simulation approach

The two fast Monte Carlo approaches used for the dose calculations read an input file which is adapted by the PODIUM application (DCA) from the RDSR file with the information described in paragraph II.1. The DCA organizes the radiation source information as it is required by each Monte Carlo programme. As an illustrative example Figure 5 shows the different input files required by MC-GPU for the simulation of each irradiation event.

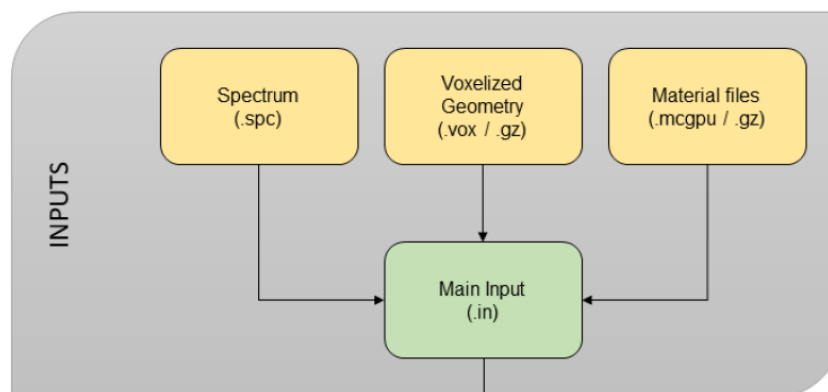


**Figure 5.** Input files required by MC-GPU.

To generate the input spectrum file, the characteristics of the X-ray tube, kVp and added filtration for each irradiation event are needed. The voxelized geometry contains the voxelized phantoms for patient and worker, and finally, the main input requires most of the other identified parameters detailed in Tables 1 and 2.

With this information, for each irradiation event, a dosimetric simulation loop is executed to calculate, in the case of MC-GPU, the worker's effective dose and organ doses. In the case of PENELOPE/PenEasy, a similar structure of input files are required, and the simulation provides the fluence distribution at a given position and subsequently fluence to dose conversion coefficients are automatically applied to obtain the operational quantities:  $H_p(10)$ ,  $H_p(3)$ ,  $H_p(0.07)$ .

Although, the calculation time is considered adequate, of the order of 60 s-90 s per event, once the calculation is validated, the sensitivity study presented in the next paragraph could be used to simplify the number of simulated cases by grouping some of the irradiation events.

## 2.4 Sensitivity study on parameters of influence

As it has been mentioned before, the scattered field that reaches the operator depends on different parameters, but it is expected that some of them will be more critical than others. The knowledge of the impact of these parameters on dose is a key factor to optimize the size of the radiation field lookup table. This analysis is also useful to assess whether the number of simulations in the fast simulation approach can be reduced.

In order to study the influence of the different parameters on the operator's radiation dose, several Monte Carlo simulations of the dose at different positions of interest have been carried out. Simulations were performed with PENELOPE/penEasy code, using the detection forcing technique described in the document "D 9.110 - Validation of the application in a controlled experiment set-up in a hospital", and the characteristics of the X-ray tube, patient's table, image intensifier... corresponding to the set-up used for the validation of the systems reported in the same document.

The characteristics of the X-ray tube taken into account to generate the beam spectra were the following:

- Anode material: Tungsten.
- Anode angle: 11.5°.
- Inherent filtration: 2.5 mm Al.
- Field size: square field of 29.7x29.7 cm<sup>2</sup> at the image intensifier (focus-intensifier-distance, 120 cm).

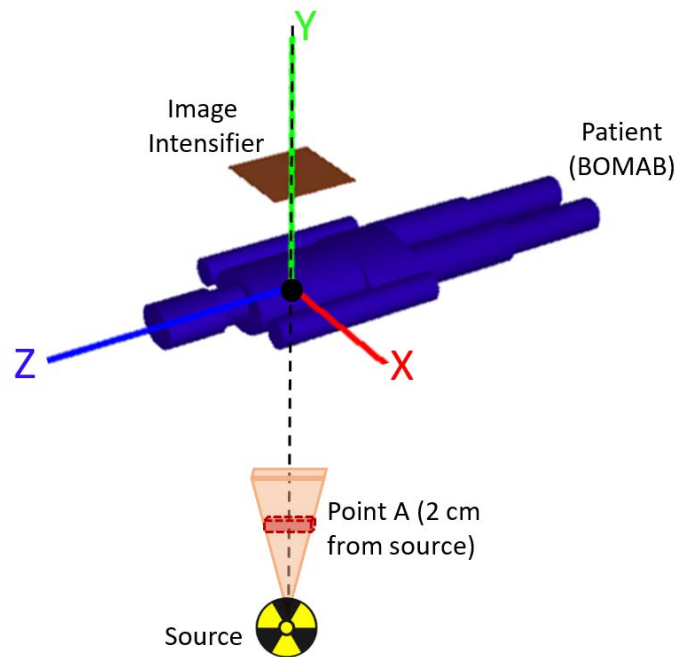
Regarding the image intensifier characteristics, it was simulated by a squared layer of 0.05 cm of CsI and a layer of 0.3 cm of Pb, located at 119.9 cm from the focal spot. The patient's table was not included in the simulation. Finally, the patient phantom was described by using a BOMAB phantom (all materials, ICRU four-components), shown in Figure 6.

The absorbed doses in air at a specified point (point A) and at different positions (P1, P2, P3, P4, P5) corresponding to different distances and heights from the focal spot have been calculated simultaneously for different kVp, added filtrations and field sizes. Table 3 and Figure 7 provide details of the location of the 'virtual' dosimeters.

In particular the following ratio was calculated:

$$\text{Ratio} \left( \frac{\text{Operator}}{\text{Reference}} \right) = \frac{\text{Absorbed dose at points (1,2,3,4,5) (Gy)}}{\text{Absorbed dose at the specified reference point (Gy)}}$$

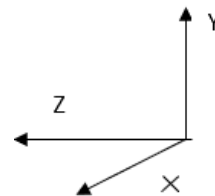
This ratio is the most interesting quantity since all simulations will be normalized to experimental values by using the dose at the reference point or the dose area product included in the RDSR files. The reference point is a virtual position defined at a specified distance from the isocenter of the C-arm. The air kerma or the dose at this point is calculated by means of the measurement of a DAP-meter located in the housing of the gantry at a fixed distance of the focal spot and using the inverse square law. In the simulations, point A was located at 2 cm of the focal spot but can be easily related to the experimental values of the DAP meter using the inverse square law.



*Figure 6. Geometric description of the patient's phantom.*

**Table 3.** Coordinates of the points of interest for dose calculations.

ELEMENT	Coordinates (cm)
Focal spot	(0.0 -78.5 0.0)
Reference point	(0.0 -76.5 0.0)
Operator P1	(38.5 28.6 -59.5)
Operator P2	(38.5 58.6 -59.5)
Operator P3	(38.5 -1.4 -59.5)
Operator P4	(38.5 -1.4 -19.5)
Operator P5	(38.5 28.6 -19.5)



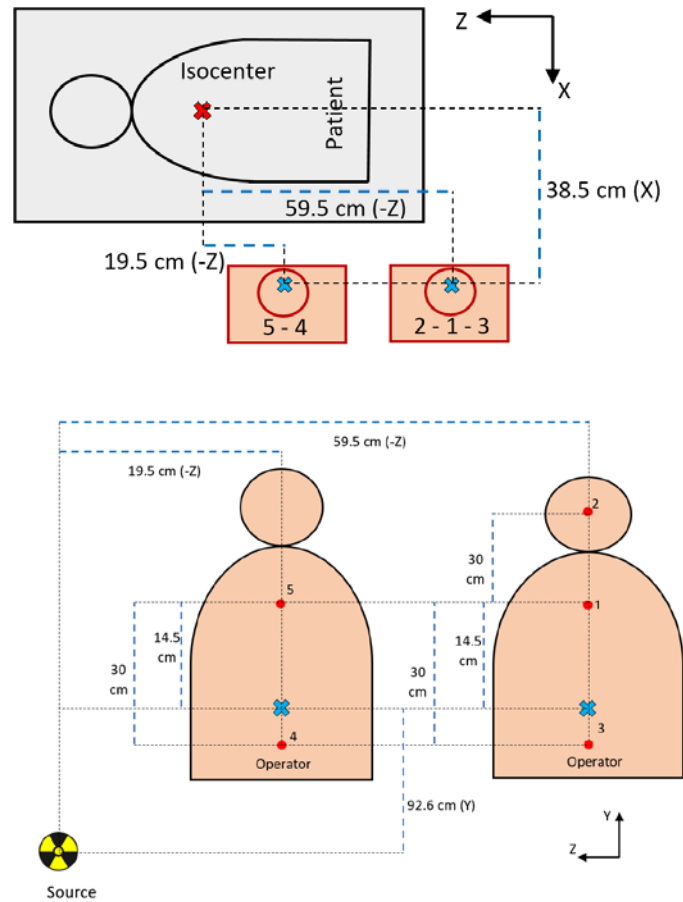


**Figure 7.** Schematic drawing of the location of P1-P5.

The sensitivity study has been carried out taking into account information from the Skåne University Hospital on the most commonly used working conditions. Figures 8, 9 and 10 show the distribution of tube voltages, added filtrations and irradiation angles in this Hospital.

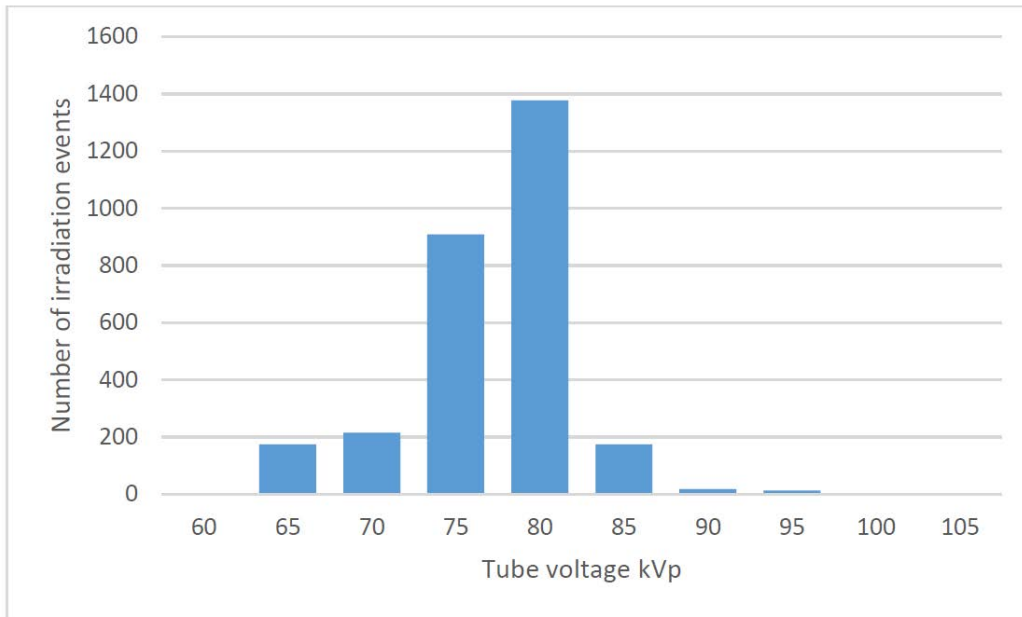


**Figure 8.** Probability distribution of used tube voltages.

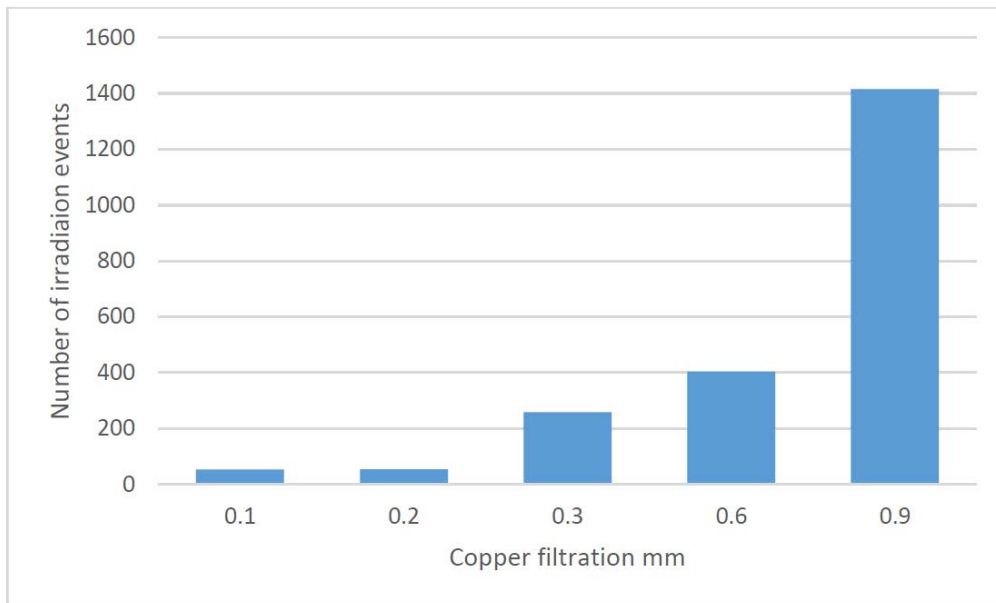


**Figure 9.** Probability distribution of applied added filtration.

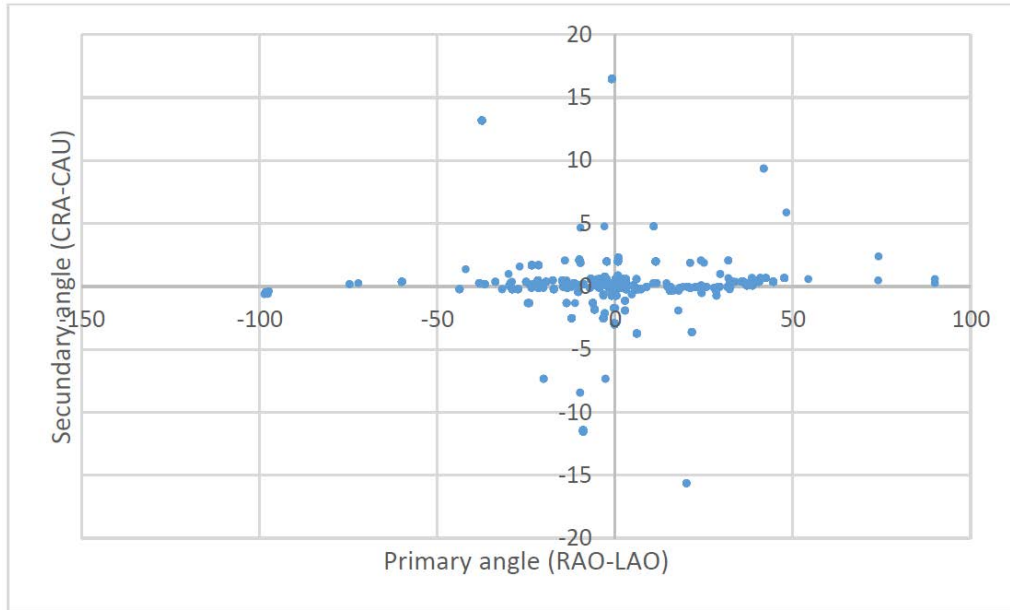


**Figure 10.** Probability distribution of used tilting angles.

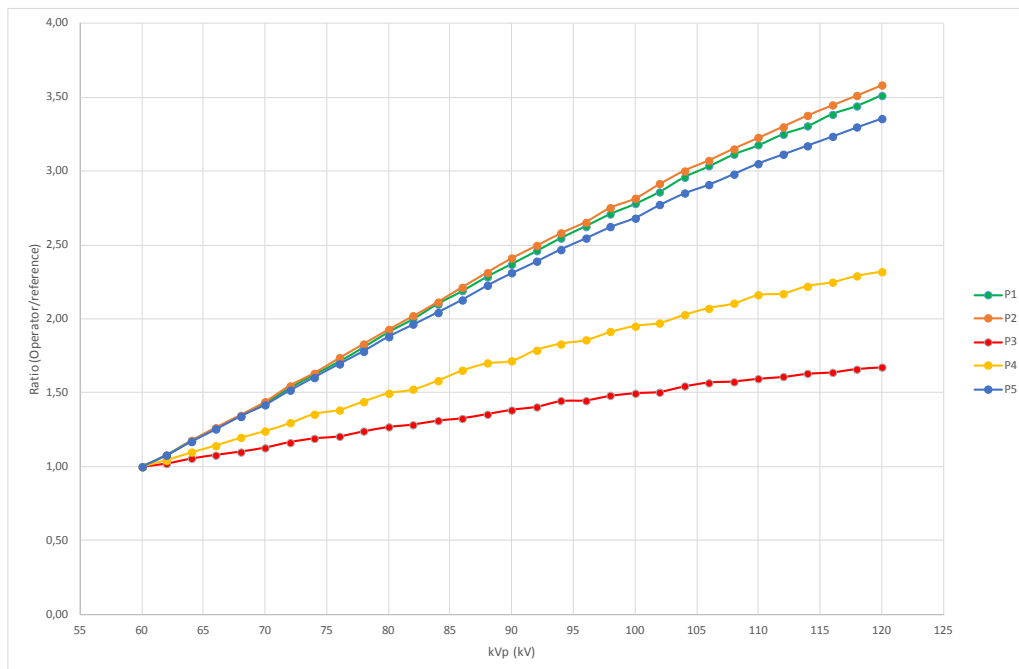


**Figure 11.** Ratio (Operator absorbed dose/Reference dose) per history vs kVp, no added filtration. Results normalized to 60 kV.

The observed tendencies for the operator absorbed dose vs added filtration and field size were similar for all studied points, thus only results for P1 are shown in Figure 12 and Figure 13.

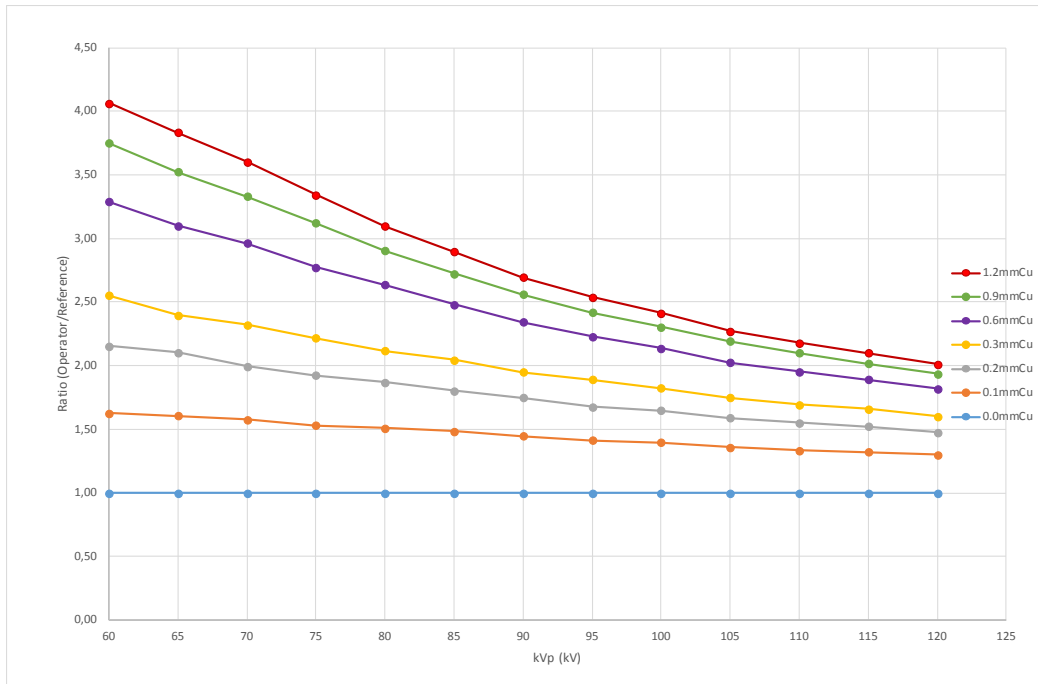


**Figure 12.** Ratio (Operator absorbed dose/Reference dose) per history vs filtration at P1. Results normalized to no added filtration.

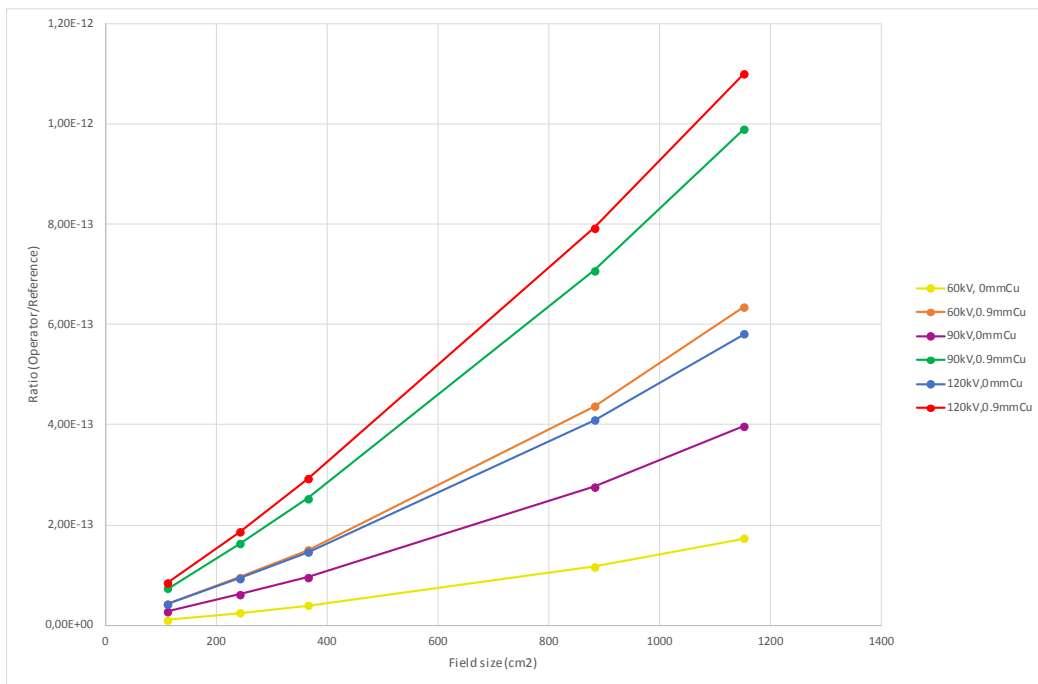


**Figure 13.** Ratio (Operator absorbed dose/Reference dose) per history vs field size, at P1.

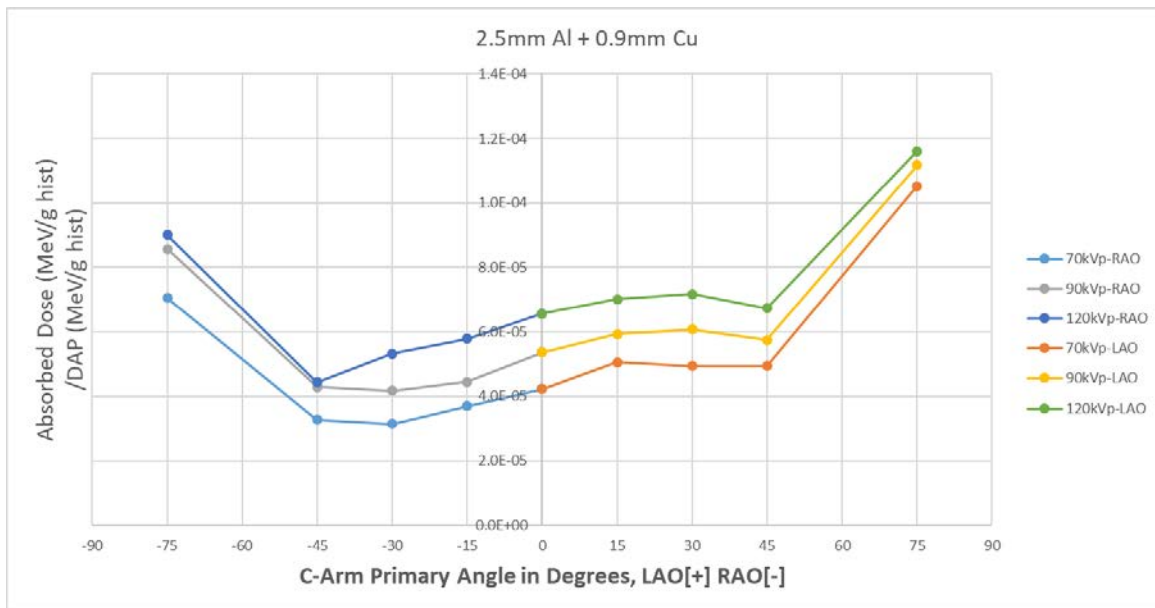


**Figure 14.** Ratio (Operator absorbed dose/DAP) vs primary angle.

The study on the influence of the primary and secondary projection angles for 3 added filtrations within the range used in practice (0, 0.2 mm and 0.9 mm of Cu) was performed with MCNPX. The absorbed dose was normalized by the Dose Area Product. In these cases, the simulations were performed with the MCNPx 2.70 particle transport code, assuming a field size of 20x20 cm<sup>2</sup> and with the dosimeter located in a position similar to P2 from PENELOPE/penEasy (see Figure 7), but closer to the patient (x-z plane) and at different height of the doctor (y-axis). In particular, the dosimeter position was extrapolated from the measurements performed in UZ Brussels hospital, resulting to be centered in (20, 49.5, -52.5).

A similar trend was observed for all the simulated added filtrations, thus Figure 14 shows the results for 0.9 mm Cu, the most commonly used filtration. The operator dose is strongly influenced by the primary rotation angle. However, within the region 45RAO – 45LAO, it is reasonable to approximate the trend with a linear interpolation.

Finally, Figure 15 shows the dependency of operator dose with secondary projection angle for the case of no added filtration. In these cases, the source-intensifier-distance (SID) was increased from 100 cm to 110 cm. This modification to the geometry was made necessary by the fact that for secondary rotations bigger than about 25 degrees (in both CRA and CAU directions), the detector would have intersected the patient body with an SID of 100 cm. An SID of 110 cm leaves a realistic clearance between the patient body and the detector, even for larger secondary angulations. The absorbed doses exhibit a nearly linear trend with the secondary angulation, at all simulated energies.

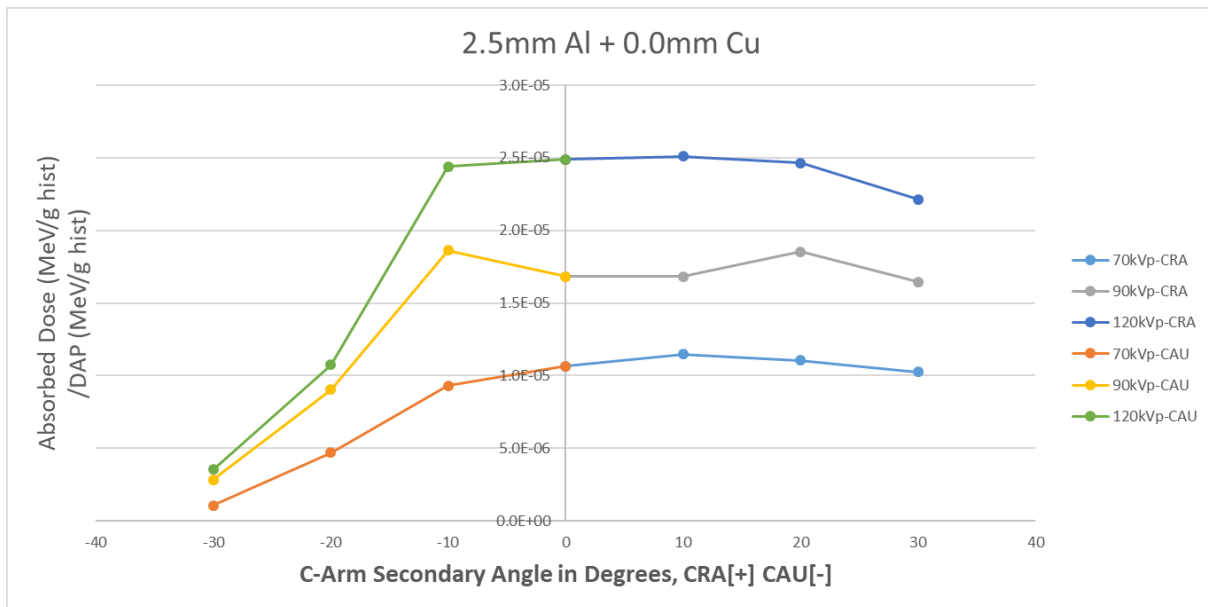


**Figure 15.** Ratio (Operator absorbed dose/Reference dose of the DAP meter) vs secondary angle of irradiation, for 70 kVp, 90 kVp and 120kVp, with no added filtration.

From the results some conclusions can be drawn:

- As regards kVp, without added filtration, the dose is quite dependent on kVp, but it can be described by a linear equation. Performing simulations every 10 kVp between 60 kV and 120kV without linear interpolation could introduce deviations of 20-50% in operator's doses.
- Regarding added filtration and kVp, Figure 9 shows that the most frequent added filtration in the clinic, are 0.9 mm, 0.6 mm and 0.3 mm of Cu. In addition the sensitivity analysis highlights differences within 15% between 0.9 mm and 0.6 mm or between 0.6 mm and 0.3 mm. For this reason, for the moment it was decided that we will simulate 4 cases of added filtration (0 mm, 0.2 mm, 0.3 mm, 0.9 mm) for the creation of the first scatter fluence files in the lookup table.
- Concerning the dependence on field size, as expected, the operator dose shows a linear dependence with the square field size value. Simulating 3 field sizes (15 cm, 20 cm and 30 cm) will allow us to reduce the total number of simulations maintaining accuracy in dose estimation.
- Finally, the dependency of operator dose with primary and secondary angulation was investigated. The results of our analysis show a complex but expected behavior, which allowed us to reduce the extent of angles to include in the first radiation field lookup table. On the one hand, by simulating 7 primary angles (90RAO, 45RAO, 30RAO, PA, 30LAO, 45LAO, 90LAO), 3 secondary angles (30CAU, 10CAU, 30 CRA) and by using interpolations between these angles, we will be able to provide accurate field characterization for any primary and secondary angles.

In total, this leads to a total number of 1764 configurations, corresponding to 7 energies, 4 thicknesses of added filtration, 3 field sizes, 7 primary angles and 3 secondary angles.

To conclude, the information obtained with this sensitivity study allowed us to define the size of the radiation field lookup table. A further optimization to reduce the number of simulations is currently under investigation. The total number of scatter fluence files will be reported in a specific document on the setting-up and validation of this approach.

## 3 Mixed gamma-neutron workplace fields

### 3.1 Radiation field mapping

The ultimate aim of the PODIUM system is to be able to perform real-time calculations of effective dose for individuals tracked by the Kinect camera. Achieving this by introducing a voxel phantom into a model of a room, and performing Monte Carlo calculations in real-time, is not possible for mixed gamma-neutron fields using current technology: the performance of the calculations, would be too slow. Moreover, this method of direct calculation is also problematic in neutron fields, due to difficulties in applying the correct radiation weighting factor to the doses deposited in the organs. As a result, the method of solution adopted by the PODIUM system is to determine in advance a set of dose rate maps appropriate for the workplace (look-up table approach), and apply those in real-time given the tracked motion of the individual. Essentially, this requires the production of appropriate dose rate conversion coefficients that are dependent on the location, posture and orientation of the individual.

It might be remarked that considering a spatial conversion coefficient map on too fine a scale might be misguided: because the body is an extended, 3-dimensional object, it is not realistic to focus solely on the dose rate at an infinitely small point. It is also not relevant to consider the effective dose at locations where an individual could not physically position themselves, such as close to the ceiling, for instance. Moreover, significant vertical dose rate gradients might exist in practical workplace fields, but most of the organs that contribute to effective dose will likely always be between ~1m and ~1.5m from the floor, notwithstanding the infinite number of stances in which an individual might pose in reality, leading to divergences from approaches based on a non-deformable phantom. Conversion coefficients at heights corresponding to a standing and a bended (or sitting person) could also be calculated if required.

For these reasons, the approach recommended within PODIUM is to map the dose rate on a horizontal grid located above the floor at the height between 1 m and 2 m at which the maximum dose rates might be expected, or else at 1.5 m from the floor if no significant vertical dose rate gradient is expected. It is assumed that this approach would provide a reasonable or conservative estimate of doses in the majority of cases. For the simulated workplace field developed at PHE, the <sup>241</sup>Am-Be source is located at 1.25 m from the floor of the facility, so this provided an obvious natural height at which to produce the dose map. In the case of the other selected workplace, a transport container with spent UO<sub>2</sub> or MOX fuel at SCK-CEN Research Centre, a larger height variation is expected because also kneeling persons can be expected and the container is situated on the floor.

The approach to the mapping is to generate conversion coefficient data, as well as dose rate magnitudes, as a function of location within the room in which the PODIUM system will be installed. Analogously to the method suggested to track objects within the facility, an (x,y) coordinate system would be overlaid onto the room, with discrete points defined within it. The simplest such approach would be a regular 1 m × 1 m grid of points extending over the whole area, but it may be desirable to increase or decrease this resolution as appropriate. The x and y dimensions of this grid also need not be equal, and the grid itself need not be uniform: more points could be clustered in the most dosimetrically relevant regions, such as close to a source where dose rates gradients might be expected to be sharpest, for instance, with fewer points likewise needing to be defined in regions where doses rates are anticipated to be more uniform. As always, choice of the most suitable grid structure would have to be made on a case-by-case basis, according to the requirements of the site in question.

With the grid defined, conversion coefficient and dose rate magnitude data would be determined for each point on it. Effective dose depends on the orientation of the individual, so in fact at each point on the grid a family of dose rate data is required; again, considering a finite set of discrete orientations,

say in  $45^\circ$  increments relative to some reference direction, would be desirable in practice. On implementation of the PODIUM system, the position of the centre of the individual tracked in real time would be interpolated to the closest position that is defined on the adopted grid and the direction that the individual is facing. The data at that point on the field map could then be used to derive the dose to the individual for the duration for which they can be considered at that location. As the individual moves, his/her position and rotation is tracked: eventually it will become closer to one of the other points on the defined grid, which would lead to the selection of a different set of appropriate values from the field map.

Although it is the effective dose to the individual that is ultimately of interest, it is recommended that also the ambient dose equivalent rate map is produced for each site.  $H^*(10)$  is preferred for the verification because, in general, neutron survey monitors response is better known.

Specifically:

**Ambient dose equivalent,  $H^*(10)$ , rate:**

The total ambient dose equivalent rate is to be determined at each location of the grid. There are two motivations for this: firstly, it allows the model to be checked against confirmatory measurements that can be made in the field using readily available instrumentation, such as hand-held survey instruments; secondly, it supports the use of installed monitors in facilities, which will be important for dose normalization and ongoing renormalization, as discussed in the next section. In theory, also a mapping purely on  $H^*(10)$  measurements is could be used. Effective doses, of course, cannot themselves be measured directly.

One way of obtaining the ambient dose equivalent map may be to define a sphere of air of radius  $r$  at each position on the grid, where  $r$  is small compared to its distance from any source (e.g.  $r \sim 10$  cm, when a  $1\text{m} \times 1\text{m}$  grid is used with its origin at the source). The contribution to  $H^*(10)$  from photons at each location may be obtained by determining the fluence-energy distribution through the sphere and convolving that by the energy dependent fluence-to- $H^*(10)$  conversion coefficients provided in ICRU Publication 57 / ICRP Publication 74, with lin-log interpolation applied at intermediate energies according to the scheme recommended by ICRU. In MCNP, for example, this is readily achieved using a binned  $f4:p$  tally in conjunction with  $de4$  and  $df4$  tally multipliers, where the binning structure is chosen to match the energy grid upon which the conversion coefficient data are tabulated. The contribution to  $H^*(10)$  from neutrons at each location may be obtained similarly, but of course using a  $f4:n$  tally, different appropriate  $de4$  and  $df4$  tally multipliers with different bin structures, and log-log interpolation. Summing the contributions from photons and neutrons provides ambient dose equivalent per source neutron; multiplying the result by the known neutron emission rate of the source leads to an estimate of the absolute value for ambient dose equivalent rate at each location.

If models of neutron survey instruments exist, such as for the GNU device that was developed by PHE, subsidiary calculations can also be performed. Specifically, the device can be placed at selected locations on the grid within the model to provide additional comparisons with measured data. This approach provides two benefits: firstly, it mitigates for the inevitable energy-dependence of response of the instrument; secondly, it mitigates for the inevitable perturbation of the field caused by the bulk of the instrument, relative to the free-in-air calculations performed for the dose map. This latter consideration may be particularly important at positions close to walls or other scattering media, where neutrons can potentially cross-scatter between the device and wall several times, depositing dose on each occasion that it is not accounted for in the free-in-air model. The existence of this phenomenon also highlights a limitation of the free-in-air approach, as individuals in the room will also be affected by this neutron ‘ping-ponging’ impact. However, the overall impact of this on individuals may likely be small in general: the effect is mostly anticipated very close to walls where individuals are perhaps less likely to be located, and is mostly caused by low-energy neutrons that contribute comparatively little to dose equivalent.

### Effective dose, $E$ , rate:

It is not possible to determine the effective dose directly, for instance by introducing a voxel phantom into the model of the room. Instead, effective dose is to be determined indirectly, by calculating the energy and angle distributions of the neutron and photon fields, as well as their magnitudes, at each location on the grid. These data can then be convolved with energy and angle dependent fluence-to-effective dose conversion coefficients, with the two components then summed to provide the total effective dose rate, subsequent to appropriate normalization.

In principle, the energies and angles should be considered as continuous variables, but in practice this would be impossible so a finite binning approach needs to be adopted. The energy binning can be achieved implicitly, however. In MCNP, for example, the dose conversion is readily achieved using  $f4:p$  and  $f4:n$  tallies in conjunction with their individual  $de4$  and  $df4$  tally multipliers, with lin-log (photons) and log-log (neutrons) interpolation schemes applied at intermediate energies. The optimal binning structure is relatively straight forward for these, with the  $de4$  and  $df4$  tally multipliers naturally binned to match the forms of the conversion coefficient data, such as the structure tabulated in ICRP 116.

The conversion coefficient dataset that is chosen will depend on the orientation of the individual. This is complicated by the expectation that in most workplace fields, the field incident on an individual will be highly asymmetric and therefore not covered by the plane-parallel, rotational, or isotropic fluence-to-effective dose conversion coefficients provided by ICRP 116.

To overcome the above limitation, a family of calculations is performed at each location on the grid, in order to calculate the directional neutron fluences in the point of interest. Consider a Cartesian coordinate system defined such that the  $(x,y)$  plane is parallel to the floor, and the  $y$ -axis can be considered an arbitrarily chosen reference direction. Consider also defining a circular region of finite size, with a radius that is small compared to the geometry of the room and grid (e.g.  $\sim 10$  cm), and such that a reference vector normal to the surface is parallel to the  $y$ -axis; it might be considered that this disc is 'facing' along the  $y$ -axis. In fact, by considering both 'front' and 'rear' surfaces of the disc, it could be described as facing both along and away from the positive  $y$ -axis ( $+y$ ).

Consider now a fluence tally binned according to the angle structure " $0^\circ, \theta^\circ, (180-\theta)^\circ, 180^\circ$ ", relative to the normal to the surface. Within the Monte Carlo code, this would separate the fluence into 3 bins of particles arriving in:

- the cone defined from  $0^\circ$  to  $\theta^\circ$
- a hollow cone defined from  $\theta^\circ$  to  $(180-\theta)^\circ$
- the cone defined from  $(180-\theta)^\circ$  to  $180^\circ$

Assuming  $\theta$  is sufficiently small, the first of these angle bins may approximate the fluence of particles incident from the 'front'. If the fluence-energy distribution of particles is then convolved with the appropriate anterior-posterior (AP) fluence-to-effective dose conversion coefficients (from ICRP116, and via a  $f4:n$  or  $f4:p$  tally in conjunction with their individual  $de4$  and  $df4$  tally multipliers), then an estimate can be derived for the forward component of effective dose. That is, if an individual were standing at that location and facing along the positive  $y$ -axis, the above approach would provide an approximate estimate of the AP component of their effective dose.

Moreover, the last of those angle bins may approximate the fluence of particles incident on the rear of an individual standing at that location and facing along the positive  $y$ -axis. So, if that fluence-energy distribution of particles were convolved with the appropriate posterior-anterior (PA) fluence-to-effective dose conversion coefficients (from ICRP116, and via a  $f4:n$  or  $f4:p$  tally in conjunction with  $de4$  and  $df4$  tally multipliers different from the AP case), then an estimate would be derived for this rear component effective dose.

Furthermore, by symmetry, if the fluence in the  $0^\circ$  to  $\theta^\circ$  angle bin is convolved with PA fluence-to-effective dose conversion coefficients, an estimate is also generated of the rear component to effective dose for an individual standing at that location but facing along the negative  $y$ -axis. Likewise, if the fluence in the  $\theta^\circ$  to  $180^\circ$  angle bin is convolved with AP fluence-to-effective dose conversion coefficients, an estimate is generated of the forward component to effective dose for an individual standing at that location but facing along the negative  $y$ -axis.

This process may be expanded further: convolving the  $0^\circ$  to  $\theta^\circ$  angle bin and  $\theta^\circ$  to  $180^\circ$  angle bin data with the left lateral (LLAT) and right lateral (RLAT) fluence-to-effective dose conversion coefficients provide the left and right components to effective dose for individuals facing along the positive  $x$ -axis and negative  $x$ -axis. Thus, from a single Monte Carlo calculation, eight results may be obtained.

The next step is to rotate the circular region about its vertical axis (i.e. parallel to the  $z$ -axis in the room) by an angle  $\phi^\circ$ , such that the reference direction becomes an angle of  $\phi^\circ$  to the positive  $y$ -axis, and repeat the procedure. This would provide front and rear contributions to effective dose for individuals facing along and away from this new reference direction, as well as left and right contributions to effective dose for individuals facing along and away from a direction that is  $90^\circ$  to it. Iterating this procedure for a range of  $\phi$  angles from  $0^\circ$  to  $360^\circ$ , and summing the different components for both neutrons and photons from the various directions, allows an estimate of total effective dose to be obtained for any arbitrary direction in which an individual might be facing. In reality, many of these calculations may be performed in parallel in the same Monte Carlo input file using multiple tallies with different *de4* and *df4* tally multipliers, so the task is not quite as demanding as might at first be thought.

The calculated directional neutron fluences in a point need to be converted to the effective dose (ICRP Publication 103) for the PHE and SCK-CEN workplaces. Therefore, for the PHE workplace the horizontal angles from  $0^\circ$  to  $315^\circ$ , in steps of  $45^\circ$  are used as broad parallel expanded beams incident on the Adult Male and Adult Female (ICRP Publication 110) phantom for the mono-energetic neutrons with energies from 1 meV to 20 MeV on the energy grid as specified in ICRP Publication 116. From these simulations organ doses are derived for both phantoms and the effective doses are calculated as recommended by ICRP Publication 103. For the SCK-CEN workplace the above calculated neutron effective dose conversion coefficients will be extended with  $45^\circ$  upwards directed beam with the same horizontal angles and neutron energies as above mentioned. For other workplaces, it might be necessary to include the same  $45^\circ$  downwards beams and may be the top down and down top directions. For this PODIUM project these other workplaces beam directions are not considered.

Thus, the dose mapping on the grid may be achieved through the use of 4 input files, which will provide effective dose rate data for individuals orientated in 8 different directions. For the PHE workplace field, these input file geometries are illustrated in Figure 16, with the cone structure also shown. The PHE facility is symmetric about the central axis, so only the lower half of the room needs to be mapped; the green blocks in Figure 16 indicate the water moderator, with the  $^{241}\text{Am-Be}$  source just to their left.

### 3.2 Use of radiation monitors for normalization

Monte Carlo codes such as MCNP provide their results relative to 'per-source-particle'. Whilst this allows relative doses to be obtained easily, normalization to the source activity (or other appropriate parameter, e.g. fluence) is necessary to obtain absolute dose rates. In environments where the rates might be changing, such a transient geographies (e.g. storage facilities) or situations where neutron fluence rates can fluctuate (e.g. accelerator facilities), it would be necessary to vary the normalization in real-time in order to derive the synchronous dose rate map. There are several ways to achieve this, the appropriateness of which could depend on a case-by-case basis.

For globally changing fields, i.e. those in which the relative dose rate at adjacent locations on the grid is fixed but the absolute magnitude at each of these can vary according to a single time-dependent scaling factor, the recommendation is to make use of an installed ambient dose equivalent monitor in the room. The response of this monitor relative to the dose rates at each location of the grid can be determined by Monte Carlo modelling, and normalized in the same way upon implementation of the PODIUM system. Any increase or decrease in the reading by this monitor from its baseline value thus provides a scaling factor that can be applied uniformly to all the other dose rates on the map. Of course, alarming capabilities could also be incorporated into this approach.

For locally changing fields, i.e. those in which the relative dose rate at adjacent locations on the grid varies in a time-dependent way, several installed ambient dose equivalent monitors would be required in the room. Use of these to provide time-dependent scaling factors would proceed similarly to the method for globally changing fields, but with different correction factors being applied on a local basis. Of course, the number of such monitors required, their locations, and which locations on the grid each would relate to, would all depend on the gradients within the room that the dose rates are expected to change with.

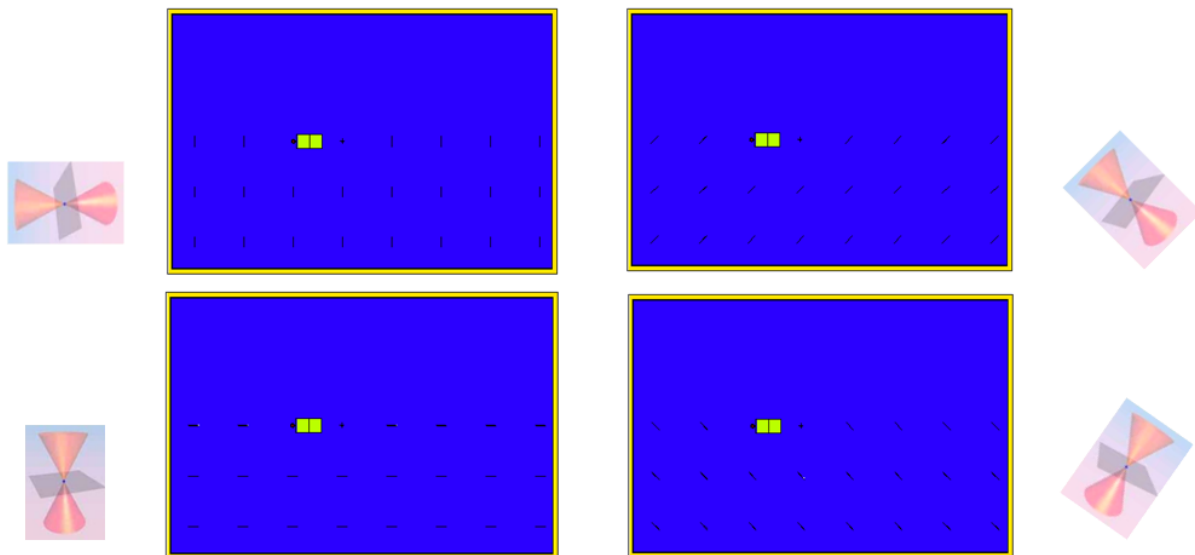


**Figure 16:** Modelled Monte Carlo geometries of the PHE simulated workplace fields, showing a 1 m × 1 m grid of tally discs, upon which angle binning is achieved using forward- and rear-facing cones. Using these four parallel input files, effective dose rate data may be achieved for 8 possible orientations of the individual at each location on the grid. A fifth input is required to determine sky-shine and floor-scatter components.

It may also be advantageous to produce a set of ‘contingency’ dose rate maps for a given environment, with the pattern of information from the various installed monitors then used to choose, in real-time, which of those maps is most appropriate at a given instance. The mechanism of applying this was discussed earlier, within the context of mitigating for facilities in which the arrangements of objects room can evolve over time. As before, the size of this set of contingency maps, and the number of installed monitors required to facilitate it, would vary on a case-by-case basis, and the judgement of the RPA and installation engineers would again be necessary to ascertain the reliability of the PODIUM system in such a circumstance.

## 4 Conclusions

This document provides guidelines on how to characterize the radiation field for either interventional radiology workplaces: C-arm, protective shields; and mixed gamma-neutron workplaces. As regards interventional radiology workplaces the required information and the foreseen data sources have been identified. In particular, for the calculations the most reliable way to gather the required information is the RDSR report. This information is of interest for the two dosimetric approaches considered in the project. The PODIUM application up-loads the information from the RDSR and transforms it to be used as input for the dose calculation. A sensitivity analysis on the impact of different parameters on the operator dose has been carried out to optimize the size of the radiation field lookup table.

For neutrons, the real time Monte Carlo method is not feasible due to the time constraints being unrealistic for such computationally intensive simulations, as well as problems with the calculation method itself. Therefore, a lookup method is used where the workplace simulations must be performed before the application of the proposed real time dosimetry system. The workplace characterization will result in lookup tables defined on grids with locational- and directional- (the facing direction of the individual) dependent effective dose conversion coefficients. This system will depend on a monitor to scale the lookup value with the instrument's reading. The lookup table is highly dependent on the workplace and the neutron sources, but can be calculated in advance using the Monte Carlo method without the time constraints of a real-time system. For these calculations to be performed detailed knowledge of the sources and workplace environment are needed. Workplaces where the presence of the individual has a strong influence on the neutron field at the worker's location have to be excluded from this real-time dosimetry proposal, as these workplaces need feedback of the worker's position before the calculations can be done with a reasonable accuracy.

## 5 References

- J. Boos, A. Meineke, O. T. Bethge, G. Antoch, P. Kröpil. Dose Monitoring in Radiology Departments: Status Quo and Future Perspectives. *Fortschr Röntgenstr* 2016; 188: 443–450.
- A. Endo. Calculation of fluence-to-effective dose conversion coefficients for the operational quantity proposed by ICRU RC26. *Radiat. Prot. Dosim.* (2016), pp. 1–10 doi:10.1093/rpd/ncw361 with supplement data.
- ICRP, 1996. Conversion Coefficients for use in Radiological Protection against External Radiation. ICRP Publication 74. *Ann. ICRP* 26 (3-4).
- ICRP, 2007. The 2007 Recommendations of the International Commission on Radiological Protection. ICRP Publication 103. *Ann. ICRP* 37 (2-4).
- ICRP, 2009. Adult Reference Computational Phantoms. ICRP Publication 110. *Ann. ICRP* 39 (2).
- ICRP, 2010. Conversion Coefficients for Radiological Protection Quantities for External Radiation Exposures. ICRP Publication 116, *Ann. ICRP* 40(2-5).
- T. Sato, A. Endo, M. Zankl, N. Petoussi-Henss and K. Niita, "Fluence-to-dose conversion coefficients for neutrons and protons calculated using the PHITS code and ICRP/ICRU adult reference computational phantoms", *Phys. Med. Biol.* 54, 1997-2014 (2009)
- T. Sato, A. Endo and K. Niita, "Fluence-to-dose conversion coefficients for heavy ions calculated using the PHITS code and ICRP/ICRU adult reference computational phantoms", *Phys. Med. Biol.* 55, 2235-2246 (2010) <https://phits.jaea.go.jp/ddcc/>